A VISCOUS MODEL OF THE EARTH

COMPARED TO GRAVITY ANOMALIES AND SEISMIC REFRACTION PROFILES

OF OCEANIC TRENCHES AND RIDGES.

W. Jason Morgan
Department of Geology
Princeton University
Princeton, New Jersey

Work done with the support of the National Science Foundation under Grant NSF-GP-1450. Supported in part by National Aeronautics and Space Administration Research Grant NsG-556.

Report No. 2; April 30, 1965

A VISCOUS MODEL OF THE EARTH

COMPARED TO GRAVITY ANOMALIES AND SEISMIC REFRACTION PROFILES

OF OCEANIC TRENCHES AND RIDGES.

W. Jason Morgan
Department of Geology
Princeton University
Princeton, New Jersey

Work done with the support of the National Science Foundation under Grant NSF-GP-1450. Supported in part by National Aeronautics and Space Administration Research Grant NsG-556.

Report No. 2; April 30, 1965

ABSTRACT

25589

The effects of a sphere and then a cylinder sinking beneath the surface of a fluid of uniform viscosity were examined. The state of the fluid at the surface is described by the "horizontal features", the horizontal velocity and the shear stress (v_x and F_{xz}), and the "vertical features", the vertical velocity and the normal stress (v_z and F_z). If the top surface is a free surface, the depression h of the surface above the sinker is related to the vertical force through the formula $F_z = \bar{\rho} g h$. It is found that F_z is independent of the viscosity of the fluid and also of the boundary conditions of the top surface -- a free surface or rigid plate give the same F_z. A two-layer model in which a fluid of one viscosity lay over a fluid of another viscosity was examined and it was found that F_z was relatively independent of the thickness of the top layer or the ratio of the two viscosities -- especially if the top layer had the greater viscosity.

The viscous model was then used to interpret oceanic trenches and mid-ocean ridges. Whereas the horizontal features are very dependent upon the assumed viscosity pattern, the vertical load F_z is not and we may find the approximate mass of the sinker and its depth beneath the surface independent of the viscosity pattern of the earth. The vertical surface load F_z was related to the thickness of the crustal layers. The variations in the crustal thickness give rise to gravity variations and these plus the attraction of the deep sinker were interpreted as the net free air anomaly. The crustal thickness ($\propto F_z$) and the free air anomaly computed for sinkers of different sizes and depths were then compared to the measured free air anomalies and seismic depths of the Puerto Rico Trench and Mid-Atlantic Ridge. In both of these cases the driving mass had an optimum depth of about 100 kilometers.

Butler

In Puerto Rico the driving mass was very concentrated at this depth: it was 5% to 10% more dense than the average density at this depth. In the Mid-Atlantic the mass was more diffuse: it was spread out over a horizontal distance of several hundred kilometers and was about 1% less dense than the average.

A VISCOUS MODEL OF THE EARTH COMPARED TO GRAVITY ANOMALIES AND SEISMIC REFRACTION PROFILES OF OCEANIC TRENCHES AND RIDGES.

1. Introduction

Runcorn (1964) has recently compared the shape of the geoid as determined both from satellite observations and surface measurements of the strength of gravity with the topographic pattern of the mid-ocean rises. He has found a correlation between lows in the geoid and the pattern of the mid-ocean rises and he interprets both of these features as manifestations of convection currents rising beneath the mid-ocean rises. The order of magnitude of this effect is correct; by assuming a uniformly viscous earth with viscosity $\eta = 10^{22}$ poise, he shows that geoid departures of 60 meters and convection velocities of 1 cm/year are compatable. Runcorn considered the global pattern of gravity highs and lows and the global pattern of convection; in this paper the gravity field surrounding a localized convection pattern will be examined.

The Fennoscandia uplift (and similar uplifts in North America) is generally assumed to be a readjustment of the earth in response to a glacial load which has recently melted. It has been assumed that the response of the crust has been governed by the laws of viscous flow and thus a measurement of the earth's viscosity has been made: the value $\eta = 10^{22}$ to 10^{23} poises is generally quoted. The following authors have considered the

Fennoscandia uplift: Haskell (1935), Vening-Meinez (1937), Niskanen (1939), and Gutenberg (1941). Haskell found $\eta = 1 \times 10^{22}$ poise, but Vening-Meinez shows an error in Haskell's assumptions and gets $\eta = 3 \times 10^{22}$ poise. Niskanen and Gutenberg both arrive at 3×10^{22} poise for Fennoscandia.

The following assumptions about the mechanics of the flow are common to all of these analyses.

(1). The crust which floats on top of the "fluid" mantle offers negligible resistance and passively follows the surface motions of the underlying "fluid".

(2). Although elastic forces may have at one time been important, only flow processes are important now.

(3). The flow is purely Newtonian viscous flow; i.e. the flow rate is strictly proportional to the shear stress.

(4). The viscosity is constant at all depths.

(5). The material is incompressible.

(6). The inertial terms in the equations of motion may be neglected compared to the term $\eta \nabla^2 \vec{v}$.

(7). The curvature of the earth may be neglected and a semi-infinite plane model used.

These assumptions are specifically listed since the same assumptions will be used in the development of this paper. The last three assumptions are readily justified, but the first four require discussion.

The assumption of constancy of the viscosity is not very good; a pattern of viscosity versus depth such as that described by Cook (1963) would be closer to reality. In the model described by Cook the viscosity has a minimum value orders of magnitude below its average value at a depth near 150 km. The evidence in favor of such a "soft layer" was recently presented by Elsasser (1964). The assumption of constant viscosity results in large motions at great depths; in the uplift models described above the vertical velocity at a depth of 1000 km (the diameter of the depressed area) is roughly one-half of its surface value. Vening-Meinez (1937) has investigated a model in which the viscosity decreased exponentially with depth. He found (for Fennoscandia) $\eta = 3 \times 10^{23}$ poise at the surface which decreased to $\eta = 3 \times 10^{22}$ at the core-mantle boundary. Takeuchi and Hasegawa (1964) have considered a model in which a thin layer of lower viscosity rests upon a fluid of much larger viscosity. They found that if the top layer were 200 km thick with a viscosity of $\eta = 1 \times 10^{22}$ poise, it would best fit the Fennoscandia data, the data for Lake Bonneville, and the apparent lag in the response of the earth's oblateness to the present length of day. A model similar to Takeuchi and Hasegawa's is reported in McConnel (1963). This assumption of constant viscosity places a serious limitation on the applicability of the results to be presented here but for mathematical convenience this assumption will be made.

A plastic model in which the stress and strain rate are not strictly proportional would be preferable to the viscous model (Orowan, 1964). One notable difference between plastic and viscous behavior is the finite strength of the plastic medium below which no flow will take place. This finite strength for the upper mantle is commonly assumed to be of the order of 10 bars. We shall examine the specific model presented here to see if this 10 bar minimum strength imposes a serious limitation to this model. We shall find that this is not too serious over a considerable volume. We shall assume that continental drift with horizontal velocities of 1 cm/ year is a proven fact and we shall find that the large density inhomogeneities required in order to produce this drift rate will produce stresses in excess of 10 bars.

The neglect of elastic forces is not very important. We have assumed that appreciable flow has taken place and in this case the elastic contribution is negligible. In the uplift problem, the crust moved only vertically and because of the large horizontal dimensions there was only a small amount of stretching or compression. In the case to be considered here, where large horizontal motions are permitted, the structure of the crust will be more important in determining the pattern of motion than in the uplift case, but for mathematical simplicity merely a thin layer "painted" on the top surface of the fluid. We shall qualitatively consider the effects of a thicker crust with strength when comparing the solution with observations.

The general equation of motion of a viscous fluid is:

$$\underset{①}{\tilde{\rho}\,\frac{d\vec{v}}{dt}} = \underset{②}{\tilde{\rho}\,\vec{g}} - \underset{③}{\vec{\nabla}P} + \underset{④}{\frac{\eta}{3}\,\vec{\nabla}(\vec{\nabla}\cdot\vec{v})} + \underset{⑤}{\eta\,\nabla^2\vec{v}} \qquad (1)$$

In this equation $\vec{g}$ is the body force per unit mass, $\vec{\nabla}P$ is the pressure gradient, and η is the coefficient of kinematic viscosity ($\eta = \tilde{\rho}\nu$). For the conditions which will be considered here, term ① is negligibly small compared to term ⑤, and term ④ is small compared to term ③. The Reynolds number, $R = \tilde{\rho}Lv/\eta$, may be calculated using a characteristic length of 100 km, a typical velocity of 1 cm/year, and a viscosity of $\eta = 3 \times 10^{22}$ poise. We find $R = 10^{-22}$. The ratio of the inertial forces to the viscous forces, the ratio of term ① to term ⑤, is always nearly equal to the Reynolds number and so the first term is completely negligible. This means we may assume that the fluid instantaneously assumes a steady state pattern: the equations are independent of time except for the motion of the boundaries. The evolution of the motion may be described by a sequence of steady state solutions. We may compare term ③ to term ④ if we know how the pressure is related to the change in volume, i.e. if we know an equation of state. If we assume $\Delta P = -k\frac{\Delta V}{V}$, then $\frac{\Delta P}{dt} = -k\,(\vec{\nabla}\cdot\vec{v})$ since $\Delta V/V$, the dialation, is equal to the divergence (of the displacement) of the material. We may now examine terms ③ and ④.

If η is constant throughout, we may write the sum of these two terms as $\vec{\nabla}[\overline{P} - \frac{\eta}{3}(\nabla \cdot v)]$, or $\vec{\nabla}(\overline{P} + \frac{\eta}{3k}\frac{\Delta P}{dt})$. The ratio η/k has the dimension of time, and for the values $\eta = 3 \times 10^{22}$ gm/cm/sec and $k = 10^{12}$ dynes/cm^2, $\tau = \eta/k$ equals 3×10^{10} sec or 1,000 years. Thus for times much longer than a thousand years we may neglect term (4) (i.e. assume $\vec{\nabla} \cdot \vec{v} = 0$) and keep only term (3). This is physically interpreted by considering the problem of an ideal "sink" at which material is annihilated at a constant rate. The first response of the neighboring material is to expand to fill this void but it cannot continue to expand forever and after a while outside material will begin to flow into this low pressure region. A steady state flow of constant mass transport across any closed surface surrounding the sink will eventually develop.

Thus we need only consider the simplified equation

$$\tilde{\rho}\vec{g} - \vec{\nabla}\overline{P} + \eta\nabla^2\vec{v} = 0 \qquad (2)$$

which is valid for the slow velocities and large distances to be considered and if we have constant viscosity. If we define $\tilde{\rho}(x,y,z,) = \tilde{\rho}_o(z) + \delta\tilde{\rho}(x,y,z)$ and $\overline{P}(x,y,z) = \overline{P}_o(z) + p(x,y,z)$ where $\tilde{\rho}_o$ and P_o are the average or "undisturbed" density and pressure at depth z, we can subtract the "z" part away and keep only:

$$\delta\tilde{\rho}\vec{g} - \vec{\nabla}p + \eta\nabla^2\vec{v} = 0 \qquad (3)$$

2. A Particular Solution

Before proceeding to the general case, let us first consider a particular problem in order to introduce the definitions and method of approach. We consider the case of a hard sphere sinking into a uniform viscous fluid.

Our first question is what need be the profile of the top surface of the fluid in order to completely cancel the gravitational attraction of the hard sphere in the space above the free surface? (We ask this question because we shall find that part of the solution for the profile of the depression produced by a sinking aphere is exactly that required to cancel gravity.) This problem has an analogy in electrostatics --- what surface charge density will accumulate on a grounded conductor in order that zero voltage will be everywhere on the other side of the wall? This problem may be solved by the method of images.

Consider the problem of a point charge q which is a distance D away from a plane wall conductor. What is the electrostatic potential at each point in space? Imagine an image charge -q situated a distance D on the other side of the wall and remove the conducting wall. The potential at each point in space is now $\phi(x,y,z) = 1/4\pi\epsilon_o(\frac{q}{r_1} + \frac{-q}{r_2})$. where $r_1(x,y,z)$ and $r_2(x,y,z)$ are the distances between the point (x,y,z) and the original and image charges respectively. At infinity and at the plane of symmetry midway between the two charges the potential is zero. At points very near the original charge the potential approaches the point charge solution $\phi = 1/4\pi\epsilon_o(q/r_1)$.

These boundary conditions are identical with those we require for the point charge near the grounded conductor wall, and by the uniqueness theorem in electrostatics the fields in region A (see figure 1) must be the same for the two cases. The field in A is really produced by the point charge and a surface charge on the wall and we may find the magnitude of this surface charge density at any point on the wall according to

$$\sigma_E = - \frac{E_{normal}}{\epsilon_o}$$

Now consider a sphere of mass $M = \frac{4\pi}{3} \Delta\tilde{\rho}\, a^3$ whose center is a distance D from the plane z = 0. Imagine a sphere of mass -M at a distance D above the plane. The gravitational field strength at the plane z = 0 is normal to the plane and has strength:

$$g_{normal} = 2 \frac{D}{(D^2+\rho^2)^{1/2}} \frac{GM}{D^2+\rho^2}$$

In analogy with electrostatics, we may define a "surface mass density" according to $\sigma_G = - \frac{1}{4\pi G} g_{normal}$. Combining these formulas we find that the required surface mass density is:

$$-\sigma_G = \left(\frac{2}{3} \Delta\tilde{\rho}\, a^3\right) \frac{D}{(D^2+\rho^2)^{3/2}} \qquad (4)$$

This surface mass density may be related to the volumetric density $\tilde{\rho}$ and a depression of the surface h_g according to $-\sigma_G = \tilde{\rho}\, h_g$. This is shown in figure 1. On the left are the mass and its image and field in all space. On the right are the mass and the surface mass density shown in formula (4). Below the plane (region A), the field is the same as in figure 1 (a), but above the plane (region B) the field is everywhere zero. This means that a surface mass deficiency as given by formula (4) will cancel out the gravitational attraction of the sphere M in the space above the surface.

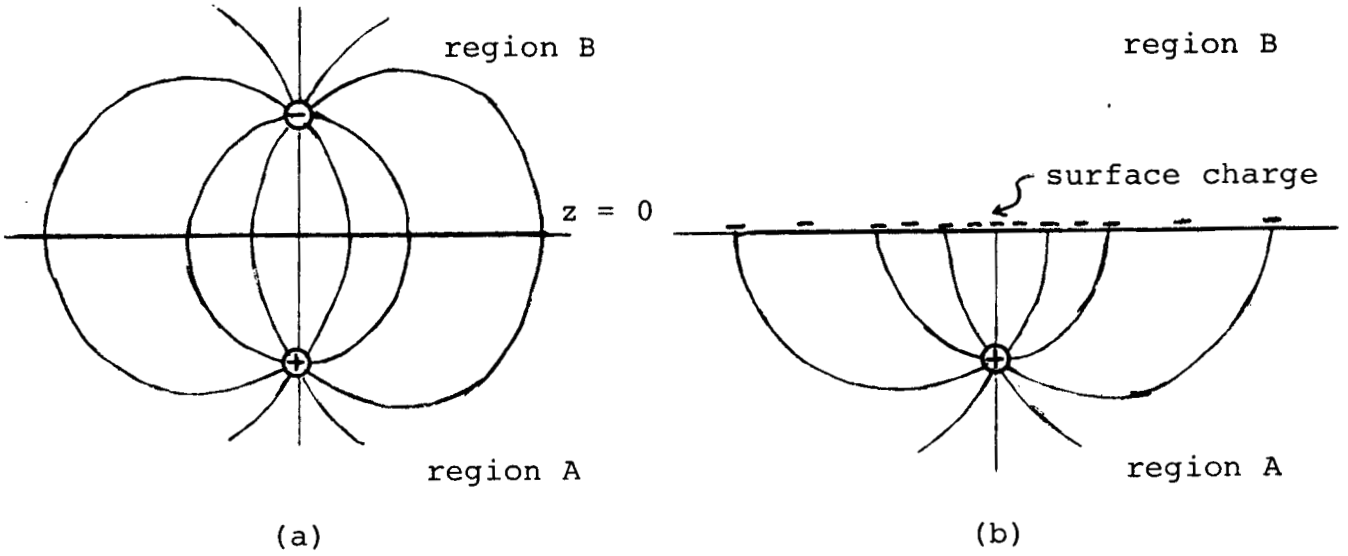

Figure 1. (a) The field of two equal but opposite point charges. (b) The field of a point charge and a chosen surface charge.

We now solve for the pressure and velocities produced by a sphere sinking in a homogeneous viscous fluid. Consider the case of a sphere of radius a falling in a medium in which $\delta\rho$ is zero. In reality the material surrounding the sinker would change density as it was dragged downward and this instability would further drive the convection, but for the moment suppose that all of the more dense material is included within the walls of the sphere.

The problem of spheres (and ellipsoids) falling in viscous media is considered in sections 335-339 of Lamb (1932) and we need only apply these results to the case of the earth. The only mathematical problem not already treated by Lamb is the effect of the free surface just above the falling sphere. Boundary conditions which closely approximate the free surface and yet which still permit a simple analytic solution will be chosen (an "image" type boundary condition) and the effects on the falling sphere will be found.

We may find the orders of magnitudes involved by considering a sphere falling in an infinite medium. In an infinite medium, the resisting force acting on a sphere of radius a and having a velocity V is:

$$R = 6\pi a \eta V \tag{5}$$

Equating this force to the buoyant force of the sphere, we have

$$V = \frac{2}{9} \frac{g a^2}{\eta} \delta\tilde{\rho} \tag{6}$$

If the radius of the sphere is 100 km and if the density is 1% of 3 gm/cm^2, then the limiting velocity is .7 cm/year. The time required for the sphere to sink 200 km (one diameter) is 30 million years. Neither a, $\delta\tilde{\rho}$, nor η are known with any precision, a factor of ten change up or down of any one of these could be possible, but the combination chosen seems reasonable and the time scale of 30 m.y. is of the order of a mountain building cycle.

The velocities in the fluid induced by the ball sinking beneath a free surface as shown in figure 2(a) are closely approximated by the velocities in the space below of figure 2(b)

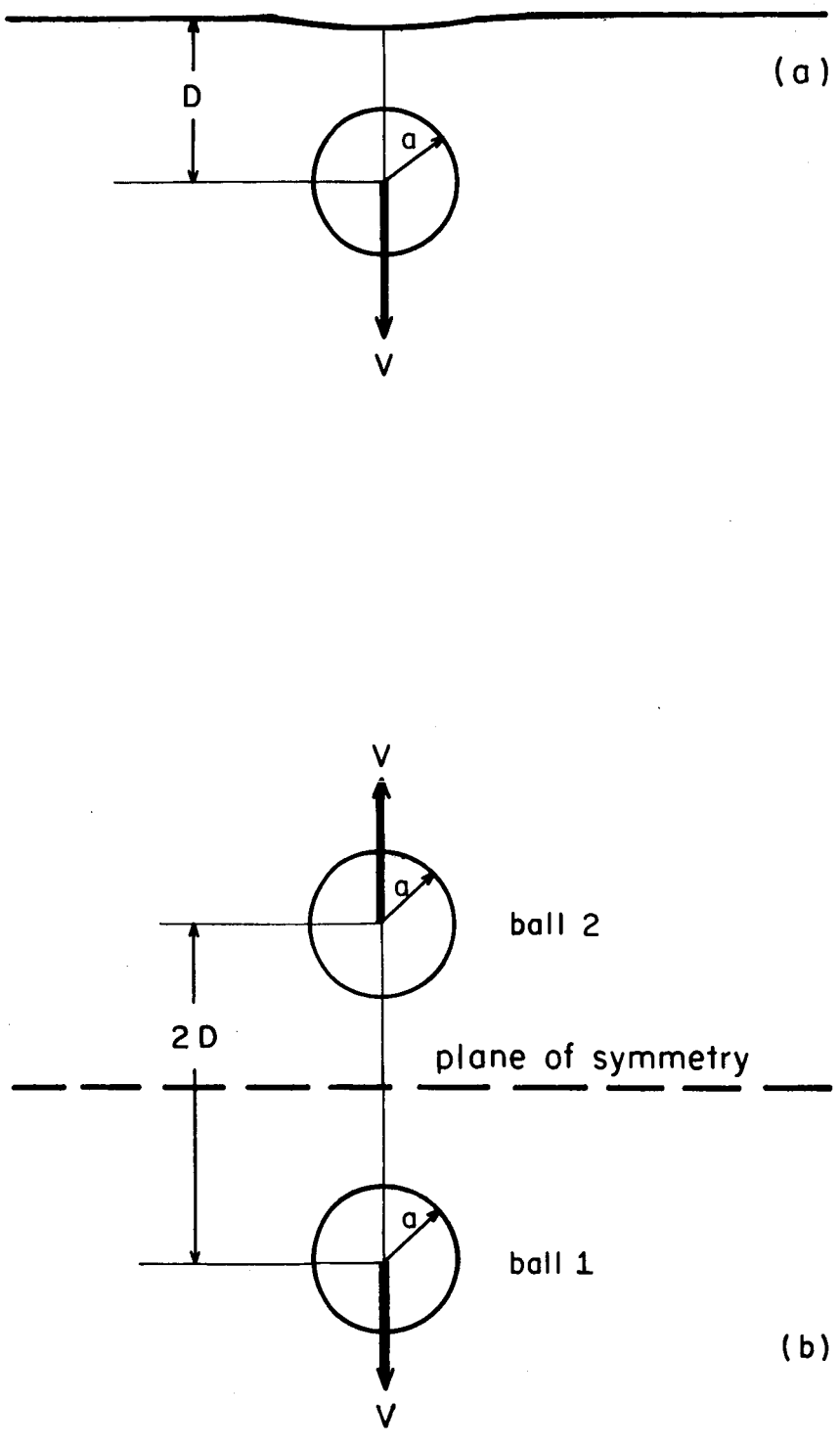

Figure 2. (a) A ball near a free surface.
(b) Two balls in an infinite medium.

in which two balls are receeding from one another in an infinite medium. The plane of symmetry closely represents the free surface as the vertical gradient in the horizontal velocity vanishes here; no tangential stresses are transmitted across this plane. The symmetry plane also strictly requires that the vertical velocity at the surface be zero and the surface be perfectly flat, but these two differences between the image boundary conditions and the actual free surface are negligible as we shall see later. Thus the problem of a ball near a free surface can be reduced to the simpler problem of two balls in an infinite medium.

To solve the two sphere problem, we may at first ignore the mutual interaction of the two spheres and represent the velocities and pressures throughout the fluid by the sum of the solutions for each ball alone in an infinite medium. This solution may be improved by a pertubation correction as outlined below. For simplicity suppose the top sphere, ball #2, is at rest and that only ball#1 is moving with velocity V. We have from the basic equation of the motion in the fluid:

$$\vec{\nabla} p = \eta \nabla^2 \vec{v},$$

$$\vec{\nabla} \cdot \vec{v} = 0$$

Thus $\nabla^2 p = 0,$

and p may be expanded in a series of spherical harmonics:

$$p = \sum_n p_n \cdot$$

Lamb (§335) shows how the velocity of the fluid may be found from different gradients of p_n's, the pressure, and ϕ_n's, arbitrary functions which are used to satisfy the boundary conditions but which do not have the same effect as pressure. Since the equations identically satisfy $\nabla^2 p = 0$ and $\nabla \cdot v = 0$ at each point in the fluid, the only problem is to match the boundary conditions. It is very easy to have $v_z = U$, $v_\rho = 0$, on the surface of ball 1, and $v_z = v_\rho = 0$ at infinity; this is just the Stokes' problem and all of the p_n's and ϕ_n's are zero except p_{-2} and ϕ_{-2}. However this does not satisfy $v_z = v_\rho = 0$ on the surface of ball #2. We may move the origin of the coordinates to the center of ball #2, find the small p_n's and ϕ_n's that are needed to satisfy the condition $v_z = v_\rho = 0$ on the surface of this ball (that is find the terms which cancel out the velocity at this surface predicted by the original solution of ball #1), and superpose this addition to the first solution. This satisfies $\nabla^2 p = 0$ throughout the fluid and $v_z = v_\rho = 0$ on the surface of ball "2 and at ∞, but it does not quite satisfy the boundary condition on the surface of ball #1 since these new terms have a small effect on ball "1. We may now return to ball #1 and find the terms which will cancel the velocities on its surface predicted by the terms just found for #2 --- this process may be continued to any desired accuracy.

For the case where both spheres are moving apart, each with velocity U, we find that the fluid velocity at each point is given by (to second order in a/D):

$$v_z = U\left(1 + \frac{3}{4}e + \frac{9}{16}e^2\right)\left\{e\frac{D}{r_1} - e\frac{D}{r_2} + \frac{e}{2}\frac{(r_1^2 - a^2)D}{r_1^3}\left[\frac{3}{2}\cos^2\theta_1 - \frac{1}{2}\right] - \frac{e}{2}\frac{(r_2^2 - a^2)D}{r_2^3}\cdot\left[\frac{3}{2}\cos^2\theta_2 - \frac{1}{2}\right]\right\} \quad (7)$$

$$v_\rho = U\left(1 + \frac{3}{4}e + \frac{9}{16}e^2\right)\left\{\frac{e}{4}\frac{(r_1^2 - a^2)D}{r_1^3}\left[3\cos\theta_1 \sin\theta_1\right] + \frac{e}{4}\frac{(r_2^2 - a^2)D}{r_2^3}\left[3\cos\theta_2 \sin\theta_2\right]\right\}$$

and the pressure by (to third order in a/D):

$$p = \frac{(6\pi U a \eta)}{4\pi D^2}\left[\left(1 + \frac{3}{4}e + \frac{9}{16}e^2 + \frac{19}{64}e^3\right)\left\{\frac{D^2}{r_1^2}\cos\theta_1 + \frac{D^2}{r_2^2}\cos\theta_2\right\} - \frac{5}{4}e^3\left\{\frac{D^3}{r_1^3}\left[\frac{3}{2}\cos\theta_1 - \frac{1}{2}\right] + \frac{D^3}{r_2^3}\left[\frac{3}{2}\cos\theta_2 - \frac{1}{2}\right]\right\}\right] \quad (8)$$

In these formulas, r_1, θ_1, r_2, and θ_2 are defined as shown in figure 3: these four quantities are always positive. Positive v_z is up and positive $v\rho$ is away from the axis of symmetry. The quantity e is defined by e = a/D; if the two spheres are touching, e = 1. The resisting force on either sphere is

$$R = (6\pi U a \eta)\left(1 + \frac{3}{4}e + \frac{9}{16}e^2 + \cdots\right) \quad (9)$$

This resistance (equation) agrees with the result of H. Dahl reported in Berker (1963) or Faxen (1927). The problem of two spheres falling alongside one another was of interest to colloidal chemists. The mutual interactions of two spheres having velocities parallel to one another (or because of the symmetry in the solution, velocities which are anti-parallel) were considered, but only the formula for the resistance (and hence limiting velocities) was published and not the pressures and velocities in the fluid nearby.

Thus the limiting velocity of a sphere of radius a, depth D from the surface, and density $\delta\rho$ greater than the fluid will fall at the rate:

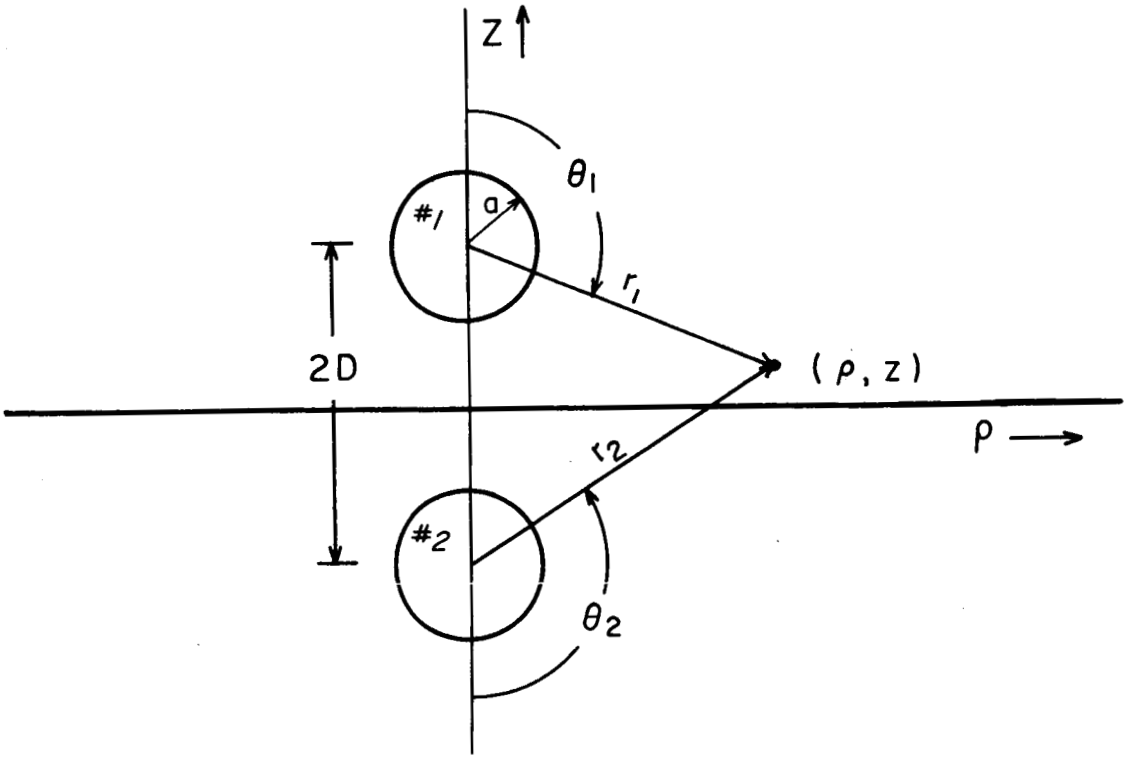

Figure 3. Definitions of symbols.

$$U = \frac{2}{9}\frac{g a^2 \delta\tilde{\rho}}{\eta}\left[\frac{1}{1+\frac{3}{4}e+\frac{9}{16}e^2+\cdots}\right] \qquad (10)$$

The horizontal velocity of the fluid along the plane z = 0 is

$$v_\rho(0,\rho) = -\frac{3}{2}\frac{a D \rho (D^2+\rho^2-a^2)}{(D^2+\rho^2)^{5/2}} U\left[1+\frac{3}{4}e+\cdots\right]$$

$$= \left[-\frac{1}{3}\frac{g\,\delta\tilde{\rho}\,a^3}{\eta}\right]\frac{D\rho(D^2+\rho^2-a^2)}{(D^2+\rho^2)^{5/2}} \qquad (11)$$

The maximum horizontal velocity occurs at about $\rho = .7D$ and is about $v_\rho = .6\,(a/D)\,U$. The pressure at the plane z = 0 is

$$p(0,\rho) = -\frac{6\pi a \eta U}{4\pi D^2}\left[1+\frac{3}{4}e+\frac{9}{16}e^2+\cdots\right]\left\{\frac{2D^3}{(D^2+\rho^2)^{3/2}}\right\}$$

$$= \left[-\frac{2}{3} g\,\delta\tilde{\rho}\,a^3\right]\frac{D}{(D^2+\rho^2)^{3/2}} \qquad (12)$$

The vertical force transmitted across a horizontal plane is in general:

$$F_z = -p + 2\eta\frac{\partial v_z}{\partial z} = -p - 2\eta\left(\frac{\partial v_x}{\partial x}+\frac{\partial v_y}{\partial y}\right) \qquad (13)$$

Evaluating this we find (dropping terms in e^2),

$$2\eta\left(\frac{\partial v_x}{\partial x}+\frac{\partial v_y}{\partial y}\right) = \left[-\frac{2}{3} g\,\delta\tilde{\rho}\,a^3\right]\left\{\frac{3D^3}{(D^2+\rho^2)^{5/2}} - \frac{D}{(D^2+\rho^2)^{3/2}}\right\} \qquad (14)$$

Thus the total vertical force (tension) at the surface may be balanced by a depression of the surface $\tilde{\rho} g h_{total}$ and we have:

$$F_z = \tilde{\rho} g h_{total} = \left[\frac{2}{3} g\,\delta\tilde{\rho}\,a^3\right]\left\{\frac{3D^3}{(D^2+\rho^2)^{5/2}}\right\} \qquad (15)$$

There are several notable features about these formulas. First, $F_z(\rho)$ and $p(0,\rho)$ are entirely independent of the numerical value of the viscosity (once η is large enough so inertial

terms may be omitted). Second, the formulas are relatively independent of the radius a of the sphere provided the density is changed to keep the mass $\frac{4\pi}{3}\delta\tilde{\rho}a^3$ constant. The pressure is independent to third order in e, the horizontal velocity is independent to second order in e (the e^2 term comes from the factor $(D^2 + \rho^2 - a^2)$, and the same e^2 dependency appears in and thus F_z.

What quantities could be measured by observing the surface of an ideal viscous fluid containing a sinking ball? From the horizontal dependence of F_z and v_ρ, the depth D could be determined. From the vertical load $F_z = \tilde{\rho}gh_{total}$, the product $\delta\tilde{\rho}\,a^3$ could be determined and an estimate of the radius a made from likely values of $\delta\tilde{\rho}$. Lastly, using the values for D and $\delta\tilde{\rho}\,a^3$, the viscosity η may be found from the magnitude of v_ρ. More information may be obtained if we observe the surface for a long period of time; if the horizontal extent of the surface pattern and thus D is observed at different times, then the limiting velocity will be known since U = dD/dt.
Equation (10) then relates U to a different combination of $\delta\tilde{\rho}$, a, and η than before, the factor $\delta\tilde{\rho}\,a^2$ appearing rather than $\delta\tilde{\rho}\,a^3$.

We now come to a main point of this paper, the relation between the gravitational attraction of the mass beneath the surface and the profile of the surface depression. Divide the total depression into two parts; the part produced by the pressure term and the part produced by the velocity term.

$$h_{total}(\rho) = h_p(\rho) + h_v(\rho)$$

$$h_p(\rho) = \left\{ \frac{2}{3} \frac{\delta\tilde{\rho}}{\tilde{\rho}} a^3 \right\} \left[\frac{D}{(D^2+\rho^2)^{3/2}} \right] \qquad (16)$$

$$h_v(\rho) = \left\{ \frac{2}{3} \frac{\delta\tilde{\rho}}{\tilde{\rho}} a^3 \right\} \left[\frac{3D}{(D^2+\rho^2)^{5/2}} - \frac{D}{(D^2+\rho^2)^{3/2}} \right] \qquad (17)$$

Notice that the pressure term (equation 16) is identical to the surface depression required to cancel out the gravitational attraction of the sphere beneath the surface (equation 4). This identity, which will be proved in general in the next section, depends upon having a medium in which viscosity is constant. However this is still "partially true" for a viscosity which varies with depth, as will be discussed in a later section.

We now examine the validity of our image method of solution. How valid is the approximation that two balls moving apart represent one ball sinking beneath a free surface? The smaller the distance h (obtained from the relation $F_z = \tilde{\rho}gh$) is compared to the depth of the ball D, the better the results calculated from the formulas above will represent the free surface case. The depth of the depression is given by (equation 15):

$$h_{total}(\rho) = H \frac{D^5}{(D^2+\rho^2)^{5/2}}$$

where

$$H = \left(\frac{2}{\tilde{\rho}} \frac{\delta\tilde{\rho}}{D^3} a^3 \right)$$

If a = 100 km, D = 200 km, and $\delta\tilde{\rho}/\tilde{\rho} = .01$, we find that the maximum surface depression is H = 5.0 m, or 1/4% of the distance D. This shows that the plane surface is a good approximation

to the slightly wavy free surface and at the same time the height of roughly a kilometer is large enough to be tectonically interesting. The symmetry of the two ball problem imposes that the plane surface z = 0 is a surface across which no shear stresses are transmitted, and we may satisfy ourselves that the free surface boundary conditions are closely met on the plane z = 0.

The second question which arises concerns the possible vertical motion of the free surface with time, a possibility which is ruled out by symmetry in the two ball problem. We may find how the time rate of H is related to dD/dt (dD/dt = U) by differentiating the formula above, and we find that dH/dt is several orders of magnitude smaller than the limiting velocity or maximum horizontal velocity. We may be assured that the image method of solution introduces no appreciable error into the solution.

3. A more general solution.

We assume that the viscosity is constant in all that follows. We will first prove the identity between P(x,y,0) and g times $\sigma_G(x,y)$ for the plane case and then discuss the case of spherical geometry.

Write the density of the fluid as the sum of two terms; a term which depends only on depth and a term which represents local departures from this average at each depth.

$$\tilde{\rho}(x,y,z) = \tilde{\rho}_o(z) + \delta\tilde{\rho}(x,y,z)$$

Now the $\tilde{\rho}_o(z)$ produces no horizontal variations in the gravity anomaly measured at the surface nor does it generate convection currents in the viscous fluid. (It may be in a situation of unstable equilibrium but only until horizontal irregularities start to occur, $\delta\tilde{\rho}(x,y,z)$, will this be of any importance.) Thus we may ignore $\tilde{\rho}_o(z)$ in the following discussion.

How do we calculate the gravity anomaly produced by the $\delta\tilde{\rho}(x,y,z)$ beneath the surface? Imagine a distribution of image masses above the plane z = 0 such that:

$$\delta\tilde{\rho}(x,y,-z) = -\delta\tilde{\rho}(x,y,z). \qquad (18)$$

We then calculate the gravitational field at the surface z = 0, use $\sigma_G = \frac{-1}{4\pi G} g_{normal}$, and find the surface mass density which will cancel the attraction of the mass irregularities below.

$$g_{normal}(X,Y,0) = G \iiint_{\text{all space}} \frac{\delta\tilde{\rho}(x,y,z)\ z}{\{(X-x)^2+(Y-y)^2+z^2\}^{3/2}}\, dx\, dy\, dz$$

Because of our extension of $\delta\tilde{\rho}$ into the upper half space according to equation (18), this integral over all space is equivalent to twice the integral over the lower half space only. Note that the above integral is equivalent to:

$$g(X,Y,0) = G \iiint_{\text{all space}} \delta\tilde{\rho}(x,y,z) \frac{\partial}{\partial Z}\left(\frac{-1}{((X-x)^2+(Y-y)^2+z^2)^{1/2}}\right) dx\,dy\,dz$$

Define $r = \{(X-x)^2 + (Y-y)^2 + z^2\}^{1/2}$. Then we have

$$\sigma_G(X,Y) = \frac{1}{4\pi} \iiint \delta\tilde{\rho} \frac{\partial}{\partial z}\left(\frac{1}{r}\right) dx\,dy\,dz \quad (19)$$

We now compute the pressure produced by this density distribution. We use the method of images and imagine the upper half space to be filled with a fluid of the same constant viscosity η and with a density as already defined by equation (18) in a uniform gravitational field pointing downwards. Thus we have

$$\eta \nabla^2 \vec{v} = \vec{\nabla} p - \delta\tilde{\rho}\,\vec{g}$$

which is valid in all space, with η and $\vec{g}$ constant and $\delta\tilde{\rho}$ with the symmetry requirements expressed in equation (18). Now take the divergence of all terms.

$$\vec{\nabla} \cdot (\eta \nabla^2 \vec{v}) = \nabla^2 p + g \frac{\partial \delta\tilde{\rho}}{\partial z}$$

The first term is zero since η is a constant and the divergence of a curl is zero ($\nabla^2\vec{v} = \nabla(\nabla\cdot v) - \nabla\times\nabla\times\vec{v}$). The vector $\vec{g}$ points in the -z direction only, so only derivatives with respect to z are present here. Thus we have

$$\nabla^2 p = -g \frac{\partial \delta\tilde{\rho}}{\partial z}$$

and from Poison's solution,

$$p(X, Y, Z) = \frac{-g}{4\pi} \iiint \frac{\frac{\partial \delta\tilde{\rho}}{\partial z}}{r} dx\, dy\, dz \qquad (20)$$

We now show that, except for a factor of g, the two integrals in formulas (19) and (20) are identical when z = 0. Note that

$$\frac{\partial}{\partial z}\left(\frac{\delta\tilde{\rho}}{r}\right) = \delta\tilde{\rho}\,\frac{\partial}{\partial z}\left(\frac{1}{r}\right) + \frac{\frac{\partial \delta\tilde{\rho}}{\partial z}}{r} \qquad (21)$$

Integrate these three expressions over all space. The integral on the left hand side is identically zero since it is the integral of an exact differential with end points equal to zero. Thus

$$\iiint_{\text{all space}} \delta\tilde{\rho}\,\frac{\partial}{\partial z}\left(\frac{1}{r}\right) dx\, dy\, dz = \iiint_{\text{all space}} \frac{\frac{\partial \delta\tilde{\rho}}{\partial z}}{r} dx\, dy\, dz$$

and we have

$$p(X, Y, 0) = g\,\sigma_G(X Y) \qquad (22)$$

Compare this with the result found in the particular case of the rigid sphere sinking in the fluid. In the case of the hard

sphere we found that to the approximation considered p was independent of e and e^2 and had only terms of e^3 or higher ($e = a/D$). See equations (12) and (8). Thus neglecting terms of order e^3, we had $p = g\sigma_c$. This was solved assuming that the sphere was perfectly rigid. We see from the above that this same relation holds (exactly) if the sphere is made up of a material more dense than its surroundings but having the same viscosity as the surrounding material. We further find that no matter what the viscosity of a fluid ball (see Lamb § 337.2), the pressure outside the ball will not be changed if the mass of the ball is kept the same, and so the relation $p = g\sigma_c$ is true irregardless of the viscosity of the sphere. We have assumed a constant viscosity everywhere in deriving this relation (equation 21), but is this too restrictive a condition? May the viscosity change across discontinuities in density? Is the less restrictive condition that surfaces of constant $\delta\tilde{\rho}$ or constant velocity should coincide with surfaces of constant η? There is the suggestion that the integral which arises if η is not constant, $\iiint \frac{(\vec{\nabla}\eta \cdot \nabla^2\vec{v})}{r} dx\,dy\,dz$, will vanish for certain viscosity-density patterns other than $\vec{\nabla}\eta = 0$, but the proof of this has not been found.

The case of spherical geometry was considered and the relation $p(a, \theta, \phi) = g_a\, \sigma_G(\theta, \phi)$ was again found to be true <u>if</u> the strength of gravity increased linearly with the radius.

Such a gravity field, $g_r = (r/a)\, g_a$, corresponds to the field inside a sphere of constant density. If g does not have this special dependence then there is an extra term in the equation but we still have an "almost identity". For the case where the density excess is concentrated at a radius b (and the appropriately larger image mass deficiency is at radius $r = a^2/b$) the additional term is proportional to the main term and we have

$$p(a,\theta,\phi) = g_a\, \sigma_G(\theta,\phi) \left(\frac{g_b\, a}{g_a\, b}\right) \qquad (23)$$

where $p(a,\theta,\phi)$ is the pressure at the surface of the sphere of radius a produced by the disturbance at r = b and its image, $\sigma_G(\theta,\phi)$ is the surface mass layer needed to exactly cancel the gravitational field produced by the mass excess at r = b, and g_b and g_a are the strength of gravity at the surface of the sphere and the strength at radius b. The angular dependence of $p(a,\theta,\phi)$ and $\sigma_G(\theta,\phi)$ are proportional in this case but the magnitudes are different from that given earlier by the ratio $(g_b a/g_a b)$. In the case of the earth where g is approximately constant in the mantle, if a density excess is located 300 km. beneath the surface, the depression of the surface produced by the pressure term is 5% larger than that required to cancel the gravitational field of the density excess. The proof of the statements made above is not shown; this proof depended upon having a fluid with constant viscosity throughout.

4. Non-Uniform Viscosity

We shall see in this section that the vertical surface load F_z (or $\tilde{\rho}\, g h_{total}$) is relatively independent of the assumed horizontal layering of viscosity for a given density distribution. This "vertical feature" and the value of the free air anomaly which is derived from the difference between the attractions of the mass at the surface and the mass below will be independent of the layering; the "horizontal features", such as the horizontal velocity at the surface or the shear stress at the surface if there is not a free surface, will be critically dependent upon the assumed layering. This means that dividing the total surface load into two parts, a "p" part and a "v" part, has a certain artificiality; each of these two parts does not preserve its identity as the viscosity is changed from uniform to a layered model whereas the sum of the two is relatively unchanged as we vary the viscosity. Nevertheless there are two points we wish to make concerning the "p" part and "v" part before proceeding to the equations with non-uniform viscosity.

The integral of $\tilde{\rho} h_{total}$ over the entire surface must be equal to the mass of the sphere or other shaped object below no matter how the viscosity varies vertically or horizontally. This is because in order to have an equilibrium situation for the longest wavelengths in this semi-infinite half space, we must have an equality between the total downward body force and the upward surface force. Second, the integral of $\bar{\rho} h_v$ over the surface will be zero regardless of the viscosity pattern below the surface if only the viscosity of the very top layer is constant. We see this from the following equations; the second equation arises by assuming η is constant over the surface and by replacing $\frac{\partial v_z}{\partial z}$ by using the relation $\nabla \cdot \vec{V} = 0$.

$$\iint_{\rho\theta} \tilde{\rho}\, g\, h_v(\rho,\theta)\, \rho\, d\rho\, d\theta = \iint_{\rho\theta} \frac{2\eta}{g}\left[\frac{\partial V_z}{\partial z}\right] \rho\, d\rho\, d\theta$$

$$= \frac{2\eta}{g} \iint_{\rho\theta} \left[\frac{1}{\rho}\left(\frac{\partial}{\partial \rho}(\rho V_\rho) + \frac{\partial V_\theta}{\partial \theta}\right)\right] \rho\, d\rho\, d\theta$$

$$= 0$$

The last integral vanishes identically if V_ρ is zero at infinity. Subtracting the integral of $\tilde{\rho} h_v$ (= zero) from the integral of $\tilde{\rho} h_{\text{total}}$, we see that the integral of $\tilde{\rho} h_\rho$ over the surface is equal to the total mass below. Thus the relation proven for uniform viscosity, $\sigma_G(x,y) = \rho(x,y,0)/g$, still has some validity since the equality of the "pressure" surface mass deficiency and the mass excess of the sinker will cause the gravitational field of these two to partially cancel each other. This cancellation will not be perfect as in the uniform viscosity case; the surface profile will not have exactly the correct shape (proportional to $1/(D^2 + \rho^2)^{3/2}$ in the case of a spherical sinker).

In the uniform viscosity case, the free air anomaly at a point was proportional to $\tilde{\rho} h_v(x,y)$ since the attraction of $\tilde{\rho} h_\rho$ and the mass below canceled out.

$$\tilde{\rho} h_v(x,y) = \frac{2\eta}{g} \frac{\partial V_z}{\partial z}(x,y,0)$$

$$g_f(x,y) = -2\pi G \tilde{\rho} h_v = \left(\frac{4\pi G}{g}\right) \eta \left(\frac{\partial V_x}{\partial x} + \frac{\partial V_y}{\partial y}\right) \qquad (24)$$

In the case of a trench or a mid-ocean ridge, we may choose the axes so that there is no y dependence,

$$g_f(x) = \left(\frac{4\pi G}{g}\right) \eta \frac{\partial V_x}{\partial x}$$

and if we integrate this along a line perpendicular to the trench we have

$$\int_{①}^{②} g_f(x)\, dx = \left(\frac{4\pi G}{g}\right) \eta \left[V_x(1) - V_x(2)\right] \qquad (25)$$

The integral of the free air anomaly across the trench should be equal to a constant times the viscosity times the difference in the horizontal velocity of the two sides. The value of this integral across the Puerto Rico Trench was -31,000 mgal·km and across the Mid-Atlantic Ridge near 35°N, + 37,000 mgal·km. Converting these numbers to cm^2/sec^2 and choosing $\eta = 3 \times 10^{22}$ poise, we find that the two sides of the Puerto Rico Trench are approaching one another at the rate of 3.5 cm/year and that the opposite sides of the Mid-Atlantic Ridge are drifting apart at the rate of 4.4 cm/year. Such an agreement between the traditional value of viscosity and the expected rates of continental drift is intriguing; but the numbers above are without significance. First, the integral $\int g_f \, dx$ depends critically on whether the free air gravity values are generally high or low in this region of the world. Puerto Rico is in an area where the readings are generally low (the geoid is depressed in the Caribbean and western Atlantic) and the North Atlantic is a region where gravity is generally high (the geoid is elevated in the North Atlantic). We assume here that such large scale regional differences in gravity, which are usually expressed as distortions of the geoid, have a different origin than the trenches and rises. Perhaps these distortions arise from convection much deeper in the mantle, but we consider that the two problems should not be mixed. Gravity line integrals across the Mid-Atlantic Ridge in the equatorial region have a zero net value and some profiles across trenches have a net positive value (e.g. Tonga Trench). Thus these gravity line integrals would have little value unless a regional average could be subtracted out. Second, this "horizontal feature" is very dependent on the assumed layering of the viscosity and the relation shown in equations (24) and (25) is true only for

the uniform viscosity case. That is the horizontal velocity of the surface is critically dependent on $\eta(z)$ whereas the free air anomaly from which the integral is made changes very little for different forms of η (z). In fact from the equality of the surface mass and the mass beneath the surface, the net integral of g_f should always be zero except for the effects of the regional average of g_f as shown by a depression or elevation of the geoid.

The trenches and rises with which we shall compare our model have a two dimensional symmetry appropriate to a cylinder sinking beneath the surface. There are two ways we may arrive at the formulas giving the surface features produced by a cylinder sinking beneath the surface of a fluid of uniform viscosity. One is to begin with the expressions for a single cylinder in an infinite medium (Lamb, § 343) and proceed analogous to the method used previously for the sphere. The second is to integrate equations (11), (12), and (15) for a series of point sources spread continuously along a line. Either way, the formulas for the surface effects of a cylindrical sinker are:

$$
\begin{aligned}
p(x,0) &= -\left(\frac{M_L g}{\pi D}\right) \frac{D^2}{D^2 + x^2} \\
F_{zz}(x,0) &= -p + 2\eta \frac{\partial v_z}{\partial z} = +\left(\frac{2 M_L g}{\pi D}\right) \frac{D^4}{(D^2+x^2)^2} \qquad (26) \\
v_x(x,0) &= -\left(\frac{M_L g}{2\pi\eta}\right) \frac{D x}{D^2 + x^2}
\end{aligned}
$$

In these formulas for the pressure, vertical load, and horizontal velocity at the surface $z = 0$, x is the horizontal distance along the surface from a point above the cylinder, M_L is the mass per unit length, and D is the depth beneath the surface of the center of the cylinder. The surface mass layer required to cancel the gravitational field produced by the mass excess

of the cylinder is proportional to the pressure at the surface, $\sigma_G = P(x,0)/g$, and so the net free air anomaly in the uniform case is

$$g_f(x) = -\frac{2GM_1}{D}\,\frac{D^2(D^2-x^2)}{(D^2+x^2)^2} \qquad (27)$$

We shall solve the two layer problem using a fourier expansion. We begin here with the fourier expansion of the one layer problem. Consider only the half space $z \leq 0$. Then since $\nabla^2 p = 0$, we may choose

$$\begin{aligned} P_k &= P(k)\cos kx\, e^{kz}, \\ p(x,z) &= \int_0^\infty P_k\, dk . \end{aligned} \qquad (28)$$

There could also be a term in p_k proportional to $\sin(kx)e^{kz}$ but we eliminate this odd term for convenience. Using the relations $\eta\nabla^2\vec{v} = \vec{\nabla}p$ and $\nabla\cdot\vec{v}=0$,

$$\begin{aligned} V_{xk} &= -\frac{P(k)}{2\eta k}(a_k + kz)e^{kz}\sin kx , \\ V_{zk} &= -\frac{P(k)}{2\eta k}(b_k - kz)e^{kz}\cos kx. \end{aligned} \qquad (29)$$

We shall also want $F_{zz} = -p + 2\eta\frac{\partial V_z}{\partial z}$ and $F_{xz} = \eta\left(\frac{\partial V_z}{\partial x} + \frac{\partial V_x}{\partial z}\right)$.

$$\begin{aligned} F_{xzk} &= -P(k)(a_k + kz)e^{kz}\sin kx \\ F_{zzk} &= -P(k)(b_k - kz)e^{kz}\cos kx \end{aligned} \qquad (30)$$

These are the general forms for the expressions for the velocities and stresses compatible with the pressure as given by equation (28). These

equations suppose that there is no mass inhomogeneity within the half space $z \leq 0$; they were derived for $\nabla^2 p = 0$. We may find the effects of a source within the medium by supposing we have a single mass discontinuity of mass per unit length M_L at $z = -D$ in an infinite uniform medium. Then we have:

$$
\begin{aligned}
P_k &= \frac{M_L g}{2\pi} e^{-k(z+D)} \cos kx \\
V_{xk} &= \frac{M_L g}{4\pi \eta k} [k(z+D)] e^{-k(z+D)} \sin kx \\
V_{zk} &= \frac{M_L g}{4\pi \eta k} [1 + k(z+D)] e^{-k(z+D)} \cos kx \qquad (31) \\
F_{xzk} &= -\frac{M_L g}{2\pi} [k(z+D)] e^{-k(z+D)} \sin kx \\
F_{zzk} &= -\frac{M_L g}{2\pi} [1 + k(z+D)] e^{-k(z+D)} \cos kx
\end{aligned}
$$

Adding the general terms to these and evaluating at $z = 0$,

$$
\begin{aligned}
P_k &= \left\{ \frac{M_L g}{2\pi} e^{-kD} + \alpha + \beta \right\} \cos kx \\
V_{xk} &= \frac{1}{2\eta k} \left\{ \frac{M_L g}{2\pi} (kD) e^{-kD} - \alpha \right\} \sin kx \\
V_{zk} &= \frac{1}{2\eta k} \left\{ \frac{M_L g}{2\pi} (1+kD) e^{-kD} - \beta \right\} \cos kx \qquad (32) \\
F_{xzk} &= \left\{ -\frac{M_L g}{2\pi} (kD) e^{-kD} - \alpha \right\} \sin kx \\
F_{zzk} &= \left\{ -\frac{M_L g}{2\pi} (1+kD) e^{-kD} - \beta \right\} \cos kx
\end{aligned}
$$

We have renamed the combinations $p(k) \cdot a_k = \alpha_k$ and $p(k) \cdot b_k = \beta_k$.

If $z = 0$ is a free surface, we must require $v_z(x,0)$ and $F_{xz}(x,0)$ to be zero for all values of x. This determines the values of α_k and β_k and thus $F_{zz}(x,0)$ and $v_x(x,0)$. But suppose that we let $z = 0$ be a rigid plate with v_z and v_x equal to zero instead. Notice that the value of $F_{zz}(x,0)$ is unchanged by these new boundary conditions: the value of $F_{zz}(x,0)$ is the same for both the free surface and the flat plate boundaries. This is shown symbolically in figure 4. In (a) we have the conditions for a free surface (V_z and $F_{xz} = 0$, v_x and $F_{zz} \neq 0$). In 4(b) we have the conditions for a flat plate boundary (v_x and $v_z = 0$, F_{zz} and $F_{xz} \neq 0$), but note that v_z and F_{zz} are identical to the shapes of v_z and F_{zz} in 4(a) above. If we had retained the odd part of p_k in equation (28), the part that contains a sin(kx) term, then we could satisfy boundary conditions as are shown in figure 4(c). We have the conditions for a free surface for all x less than zero and the conditions for a flat plate for x greater than zero. Yet F_{zz} and v_z are the same as in (a) and (b). This has great significance to the problem at hand. We see that the effects of a rigid crust are insignificant if we are interested in F_{zz}, although these are important if we wish to know v_x.

We have just used $F_{zz}(x,0) = 0$ and $v_z(x,0) = 0$ as the boundary conditions for a free surface at $z = 0$. These are really the exact boundary conditions for two cylinders moving symmetrically apart, but as we have seen before they are a very good approximation to the free surface.

We shall now find the fourier expansion for a layer rather than a half space. For simplicity suppose there is symmetry about the x axis and that we are interested in the region $-d \leq z \leq +d$ with symmetry about $z = 0$. We shall have no mass sources within this layer, all of the sources are in the half space below, and so we find:

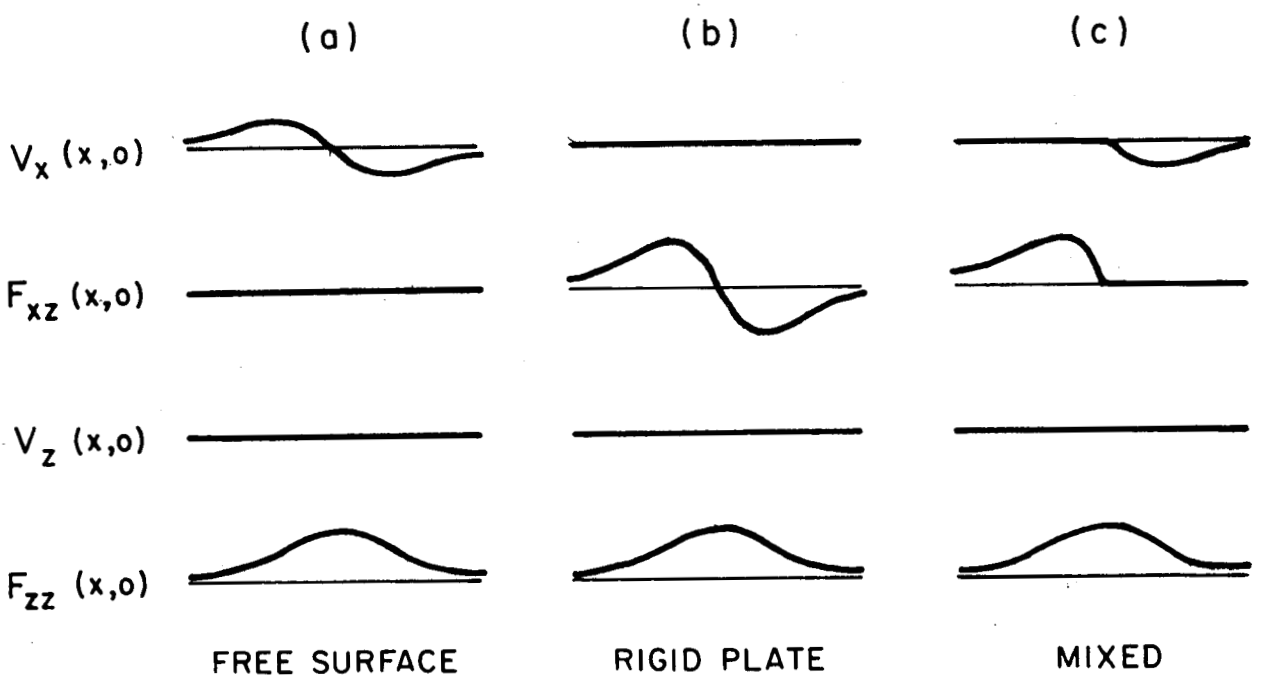

Figure 4. Symbolic diagram showing the independence of $F_{zz}(x)$ upon the choice of boundary conditions at the surface.

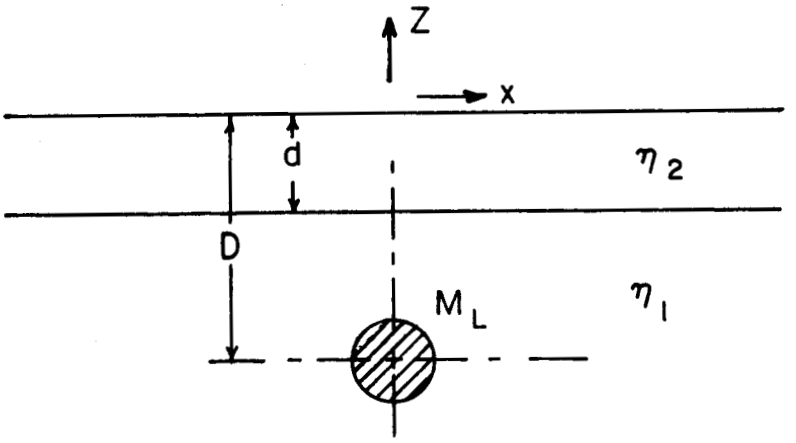

Figure 5. Geometry of the two layer problem.

$$
\begin{aligned}
p_k &= p(k)\ (\cosh kz)\ \cos kx \\
v_{xk} &= -\frac{p(k)}{2\eta k}\ (kz \sinh kz + a_k \cosh kz) \sin kx \\
v_{zk} &= -\frac{p(k)}{2\eta k}\ (-kz \cosh kz + b_k \sinh kz) \cos kx \\
F_{xzk} &= -p(k)\ (kz \cosh kz + a_k \sinh kz) \sin kx \\
F_{zzk} &= -p(k)\ (-kz \sinh kz + b_k \cosh kz) \cos kx .
\end{aligned}
\tag{33}
$$

Examine the geometry as shown in figure 5. We must match v_x, v_z, F_{zz}, and F_{xz} on the surface z = -d. Combining equations (32) and (33) we have for F_{zz} on the surface z = 0:

$$
F_{zz}(x,0) = \int_0^\infty F_k \cos kx\, dk ,
$$

where

$$
F_k = \frac{M_L g\, e^{-k(D-d)}}{RS+C} \left\{ 1 + k(D-d) + kd\left[\frac{1 - kD + k(D-d)\frac{RC+S}{RS+C}}{1 + \frac{kd\,(1-R^2)}{(RS+C)(RC+S)}} \right] \right\} \tag{34}
$$

We have let $R \equiv \eta_1/\eta_2$, $C \equiv \cosh kd$, and $S \equiv \sinh kd$.

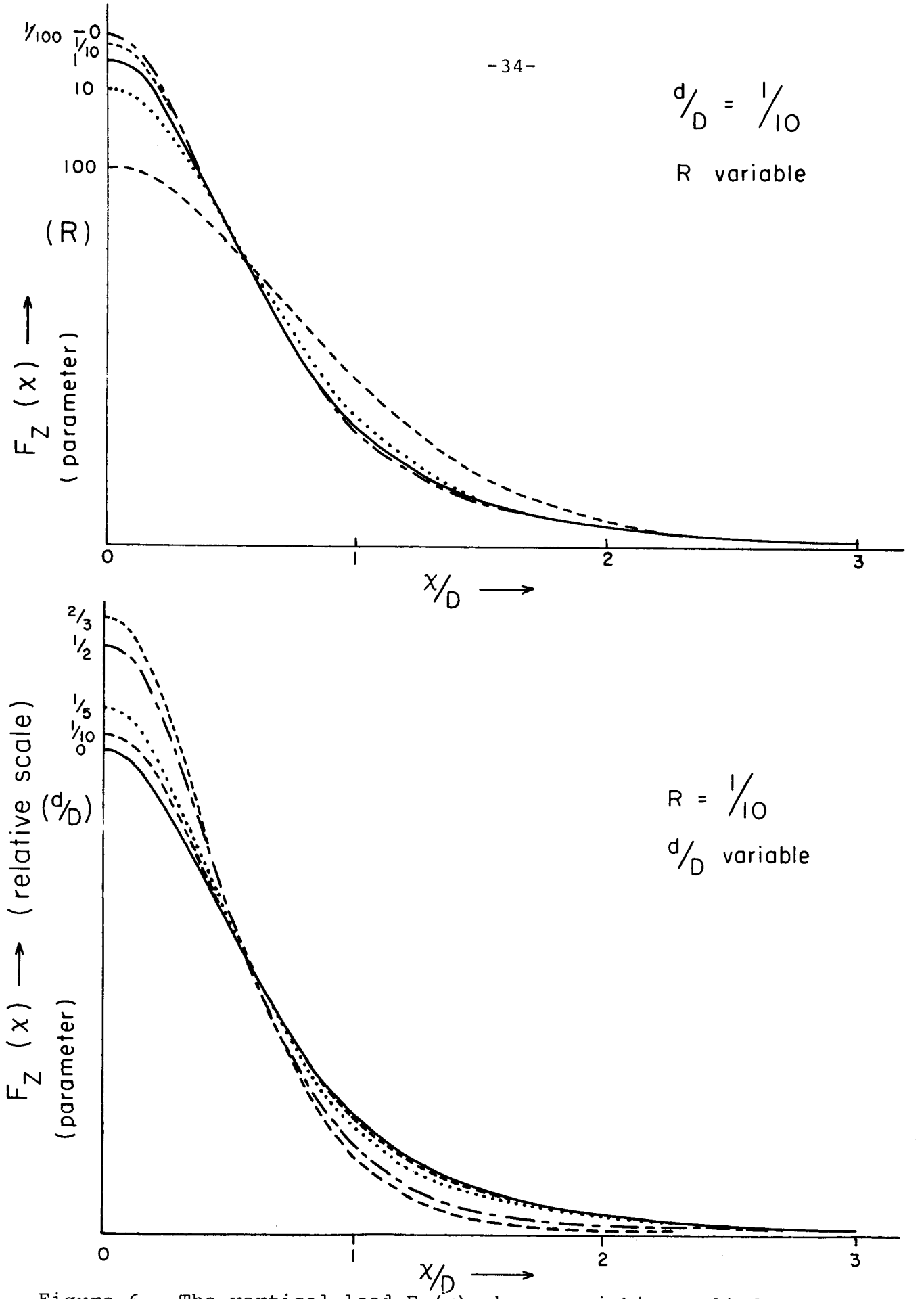

Figure 6. The vertical load $F_z(x)$ above a sinking cylinder computed with the two-layer model for various ratios of the viscosity ($R = \eta_1/\eta_2$) and various ratios of the thickness of the top layer d to the depth of the cylinder D.

This equation was integrated numerically for different combinations of the ratios $R = \eta_1/\eta_2$ and d/D. The resulting curves of $F_{zz}(x)$ are shown in figure 6. In the top part of this figure the ratio d/D was kept at 1/10 and the parameter R was varied. Note that the curve $F_{zz}(x)$ is independent of any particular value of η_1 and that the area under each curve is constant (proportional to M_L). The curves tend to peak up at x = 0 as the viscosity on top increases and there is a limiting shape of $F_{zz}(x)$ as the ratio R approaches zero. There is no limiting shape of F_{zz} as the viscosity on top decreases -- the surface load spreads out thinner over a larger area. In the bottom part of this figure the viscosity ratio $R = \eta_1/\eta_2$ was kept at R = 1/10 and the ratio d/D varied. The curve $F_{zz}(x)$ seems to be bounded for any choice of d/D.

Since $F_{zz}(x)$ is independent of any particular value of the viscosity and since the shape of $F_{zz}(x)$ is relatively independent of the vertical distribution of viscosity (at least if η increases towards the surface), we may find the mass below which produces a given surface load with a minimum of knowledge about the viscosity of the upper mantle. We shall originally assume that $F_{zz}(x)$ has the shape as given in the uniform viscosity case and later shall suppose it has the more peaked up shape of a case in which there is a thick top layer of much greater viscosity than below.

5. Comparison with Observation.

A basic feature of the viscous model is that the ocean trenches are produced by a large mass sinking deeper into the mantle many tens of kilometers beneath the trench and that the mid-ocean rises are produced by lighter material rising beneath the rises. In this section two such regions of the earth, the Puerto Rico Trench and the Mid-Atlantic Ridge, will be compared to the predictions of the viscous model.

We have seen that the "horizontal features" of the surface, such as the horizontal rate of drift at the surface, are critically dependent on the assumed layering of the viscosity of the mantle. However the "vertical features", such as the vertical surface load or the gravity anomaly, were shown to be relatively independent of the particular viscosity layering chosen. Because of this insensitivity, the results of the simple uniform viscosity model may be considered to be a good first approximation to the more exact solution.

There are three types of data with which we may compare the theory. The first is the "subcrustal gravity anomaly", g_s. Suppose that the free air anomaly is known. Further suppose that the crustal structure is known -- i.e. the depth to each interface and the density of each layer. We may use the simple flat plate approximation to compute the gravitational attraction of these crustal layers, $g_c(x) = \{ 2\pi G (\tilde{\rho}_1 \Delta h_1(x) + \tilde{\rho}_2 \Delta h_2(x) + \cdots) - \text{constant} \}$. We then determine the gravity anomaly produced by masses deep within the mantle by taking the difference between the measured free air value and the accounted for, crustal, value: $g_s(x) = g_f(x) - g_c(x)$. In the mid-oceanic areas, this subcrustal anomaly will be very similar to the Bouger anomaly since the free air anomaly is almost zero and most of the

crustal effect will be due to the water-basement interface. If the crustal structure is known so that $g_s(x)$ can be determined, then there is a powerful constraint on the form which the mass distribution below the crust may assume. One other constraint, such as specifying that the mass inhomogeneities all occur within a layer a specified distance down, is all that is needed to determine a definite density pattern for the deeper mass. The inferences derived from the quantity g_s have the great advantage that they are independent of the particular plastic or viscous model used -- gravity depends only upon mass distributions and not the rheological properties of the medium.

A second quantity which will be used is the "vertical surface load", F_z. This quantity also requires a knowledge of the crustal structure before it can be calculated. The load of a mountain or island is distributed over its entire base area, but we shall ignore this spreading effect and compute F_z at a point by summing the weight of all of the masses above it: $F_z = \{(\bar{\rho}_1 g \Delta h_1(x) + \bar{\rho}_2 g \Delta h_2(x) + \cdots) - \text{constant}\}$. This quantity is proportional to the crustal gravitational attraction g_c defined before, and again an arbitrary constant has been removed in order to make this quantity equal to zero at distances far from the trench or rise. The simple viscous model predicts the F_z resulting from a given density distribution in the mantle. Thus for a known F_z, we may again infer upon the mass distribution beneath the surface, but this time our inference does depend upon the validity of the simple viscous model.

There is a third measured quantity which will be used in the comparison, the free air anomaly, g_f. The viscous model predicts the form of the surface load F_z which manifests itself in the form of density differences in the crust. The gravitational attraction of the crustal density variations, g_c, plus the

attraction of the driving mass deep within the mantle combine to form the net gravity field, g_f. Again we may infer what the distribution of mass beneath the surface is from a surface measurement; again the accuracy of our inference depends upon the reliability of the simple viscous model.

The three quantities g_s, F_z, and g_f are not independent. The subcrustal gravity anomaly g_s has special significance in that it is independent of the viscous or other model chosen. The free air anomaly g_f has the advantage that no knowledge of the crustal structure is required, only a surface gravity profile. The quantity F_z is redundant. It can be obtained from the difference of the other two quantities, but it will be retained because of its direct physical interpretation. We shall later modify the viscous model to better account for all data and this modification is best interpreted as a change in the shape of the $F_z(x)$ produced by each piece of mass beneath the surface. We shall be interested only in surface profiles perpendicular to long trenches or rises and in this two-dimensional geometry the three quantities of interest are related to the mass beneath the crust according to:

$$
\begin{aligned}
g_s(x) &= \frac{2GM_L}{D}\left(\frac{D^2}{D^2+x^2}\right) \\
F_z(x) &= -\frac{2gM_L}{\pi D}\left(\frac{D^4}{(D^2+x^2)^2}\right) \\
g_f(x) &= -\frac{2GM_L}{D}\left(\frac{D^2(D^2-x^2)}{(D^2+x^2)^2}\right)
\end{aligned}
\qquad (35)
$$

The vertical load F_z is positive for a compression. The quantity F_{zz} which was used before was positive for tension, i.e. $F_{zz} = -F_z$. The quantity M_L is the mass per unit length at a distance D beneath the surface; x is the

horizontal distance along the surface measured from the point directly above the mass M_L. The G and g are the Newtonian gravitational constant and the acceleration of gravity respectively.

We shall call the predictions made by equations (35) above the predictions of the "simple viscous model." The basic assumptions of this model are that the mantle has a uniform viscosity and the surface load manifests itself as a thin layer of different density at the surface.

The Puerto Rico Trench is one of the most thoroughly studied regions of the earth with closely spaced gravity stations and a large number of seismic refraction lines which give the depths to different discontinuities in the crust. A north-south profile across Puerto Rico showing the seismic refraction and gravity data is reproduced in figure 7. A map showing the location of the seismic lines in relation to the gravity profile is shown in figure 8. These figures are from Talwani, Sutton, and Worzel (1959).

Talwani, Sutton, and Worzel have interpreted this data in the following way. The seismic data was used to determine the depths to all of the crustal interfaces, and an experimental velocity-density relation was used to assign a density to each of these upper layers. They then assumed that the lowest crustal layer, the layer in which the 7.0 km/sec velocity was measured, has a uniform density of 3.0 gm/cm^3, and that all material below the Mohorivicic discontinuity has a density of 3.4 gm/cm^3. With these restraints (and with knowledge of the depth to the Moho at one point on the outer ridge) only one unknown remains; the profile of the $\tilde{\rho} = 3.0$ and $\tilde{\rho} = 3.4$ gm/cm^3 interface. The gravity effects of the upper, known, layers were computed and then this unknown profile, which they call M, was adjusted so that the total computed gravity anomaly agrees with the measured gravity anomaly. The dots in the lower part of figure 7 are the gravity measurements, and the solid line is

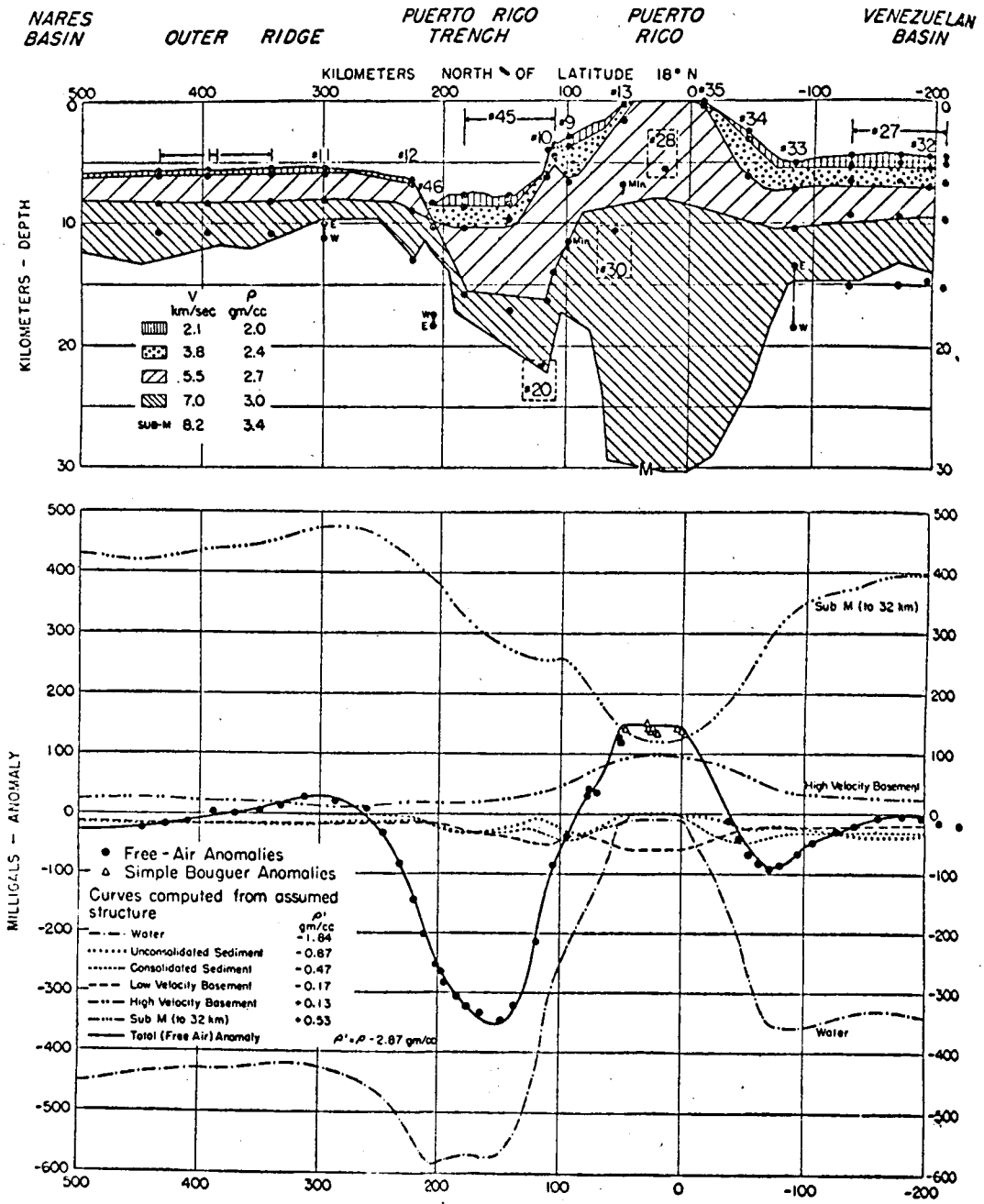

FIG. 3—*Upper*—Computed crustal section. Crustal layering is from seismic data; M is from gravity data; points are seismic interfaces. *Lower*—Computed attraction of layers to 32-km depth using reduced densities ρ'. Solid curve is total attraction (computed free-air anomaly) which is compared with observed anomalies.

Figure 7. (From Talwani, Sutton, and Worzel; 1959)

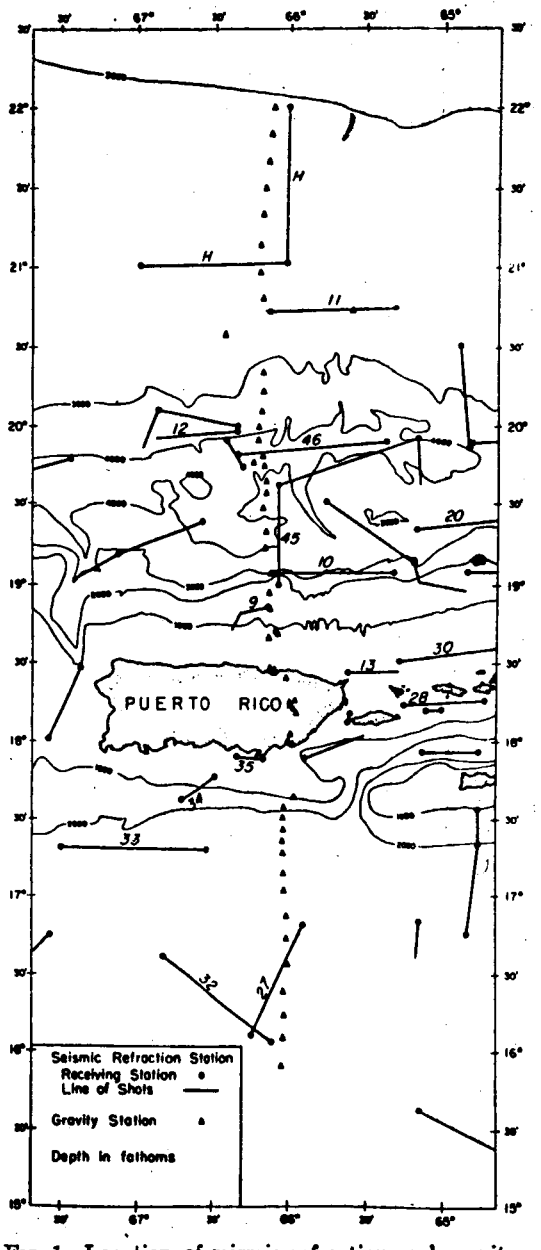

FIG. 1—Location of seismic refraction and gravity stations.

Figure 8. (From Talwani, Sutton, and Worzel; 1959)

the gravity computed using the crustal structure shown in the upper part of this figure. Near the edges of the figure the interface M agrees with the seismic refraction data, but remember that one depth had to be fed into the model since the gravity data alone is quite insensitive to the depth on any large flat layer. In the region where M undergoes large changes, from about -100 km to +200 km, there is only one seismic data point, line #20 which was measured more than 100 km off to the east of this profile. (Distances are to be measured north from latitude 18° N.) See figure 8. The significance of line #20 will be discussed later in connection with the Moho profile shown in figure 12.

Talwani, Sutton, and Worzel's interpretation of the gravity and seismic refraction data near Puerto Rico is the only sensible interpretation <u>if</u> there are no density variations in the material beneath the Moho. But even though such a structure of depths to interfaces and density of layers will account for the observed seismic and gravity data, there still remains a serious problem of dynamic instability. If this gravity low is produced by having light crustal materials extending down to roughly 20 km beneath the surface as shown in figure 7, then there are tremendous forces which will try to lift the trench floor until an equilibrium situation is reached and the trench no longer exists. That is, although the structure shown in figure 7 will explain the observed gravity and seismic data, such a structure is possible only if the trench floor and surrounding regions are rising rapidly, say at a few cm/year, or if the crustal and mantle rocks have a very great strength. For an idea of the magnitude of the stresses involved, consider the following schematic representation of this region. Suppose the Puerto Rico gravity anomaly is produced by a long prism beneath the surface with a width, w, of 100 km and a height, h, of 10 km. Suppose that the free air anomaly is zero

except right over this prism where it is -250 mgal. Using the simple formula $\delta g = 2\pi G \tilde{\rho} h$, we find that the density deficiency of this prism should be $\Delta\tilde{\rho} = -.6$ gm/cm^3. This plug must be held down by a tension on the bottom surface or a shear on the two exterior sides (cylindrical geometry). Matching the excess surface forces with the excess body force we have: $Tw + 2Sh = \Delta\tilde{\rho} hwg$. If we suppose that the tension and the shear stress are equal, then we find that $T = S \approx 500$ bars. A stress of this magnitude is at the limit of what rocks can withstand.

If we remove the constraint that the density below the Moho has no inhomogeneities, then the problem no longer has a unique solution. But if we suppose that many tens of kilometers below the gravity low there is a heavy mass which is slowly sinking deeper into the mantle, then we have a mechanism which preserves the gravity low at the surface for millions of years rather than with a time scale of tens of thousands of years as in the case of Fennoscandia or Lake Bonneville. Once the dimensions of the large subterranean mass are decided upon as required to keep the profile of the trench in a steady state equilibrium, then the profile of the Moho can be uniquely chosen in order to match the measured gravity anomaly, if indeed a sharp Mohorivicic discontinuity does occur beneath trenches. The relation between the steady state pattern of the surface and the dimensions of the "sinker" will depend on the relationship between strain rate and stress, but for simplicity assume that the simple viscous relation is true.

There is an asymmetry in the gravity profile of the Puerto Rico Trench -- such an asymmetry is present in all trenches -- and the correct solution should probably include an asymmetric convective motion slanting downward under Puerto Rico from the Atlantic toward deep under the Caribbean. However we may remove most of the asymmetry of the trench by considering that the

total observed gravity profile is the sum of two parts: a part produced by an island in isostatic equilibrium plus the effects of the trench. See figure 9.

An island in isostatic equilibrium has a gravity profile similar to that shown in figure 9b). Directly over the island, the gravity anomaly is very positive since there is much more rock and less water beneath the surface than elsewhere in the ocean. But if the island has existed a long time and is in isostatic equilibrium, then there must be a large "root" of less dense material beneath it in order that the island plus root can float like an iceberg in the denser mantle. This root is the cause of the lower than normal gravity anomaly in the seas adjacent to the island. Isostatic equilibrium is achieved when the integral of the free air gravity anomaly over the entire area is zero. Over a small area isostatic equilibrium does not occur because of the strength of the crustal material, but over areas of a radius of roughly 100 km this isostatic equilibrium is the general rule -- the most important exceptions to this rule are the trenches. In the usual example of one island in the middle of the ocean (radial symmetry), the island has a large positive g_f and the surrounding seas have a small negative g_f. However Puerto Rico has a two dimensional symmetry, the Virgin Islands on the east and Hispaniola on the west rise essentially the same height from the ocean floor as does Puerto Rico, and in this geometry the line integral of $g_f(x)$ integrated along any straight line crossing the island should have a net value of zero.

The assumed "isostatic island" shown in figure 9b) was obtained in the following manner. The gravity measurements listed in table 2 of Talwani, Sutton, and Worzel (1959) were used with the exception of minor changes in the values for the land stations. The values measured on land were changed

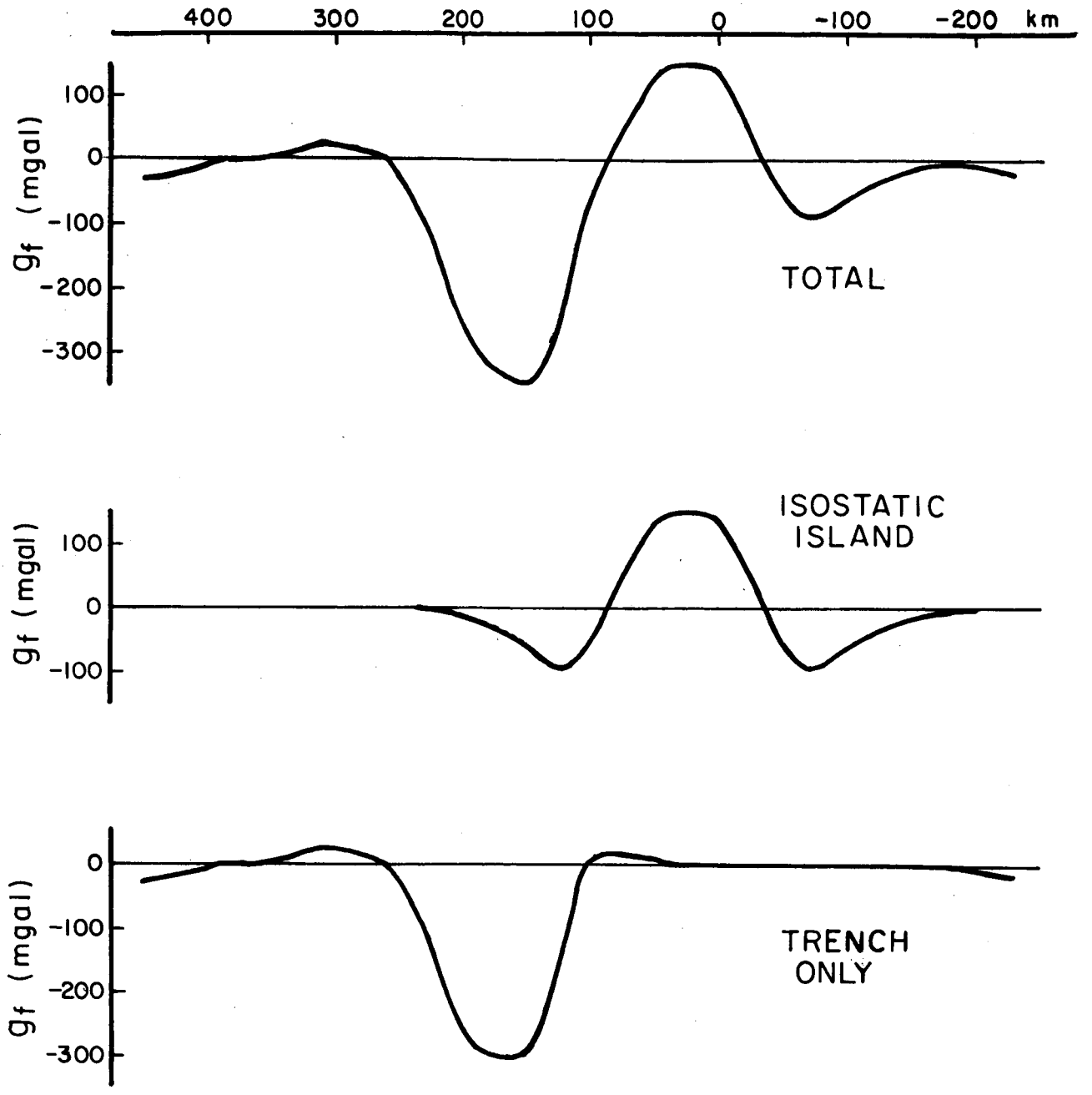

Figure 9. The free air anomaly of Puerto Rico decomposed into two parts: a symmetrical "isostatic island" and the remaining "trench only".

to free air values using the heights and density given by Talwani, Sutton and Worzel instead of the simple Bouger values tabulated in table 2. These gravity values, which were measured at irregular intervals along the profile, were then converted into values spaced every 10 km by interpolation. The accuracy of the measurements is so good that a linear interpolation between the adjacent measurements was quite sufficient -- an exception to this rule was made for the value at +50 km where three values were used to graphically determine the value of $g_f(+50)$. This equispaced data was then used in all computations rather than the original data. This data is shown in figure 9(a). The negative area between -35 km and -180 km was then found: -6010 mgal·km. The positive area under the island north of -35 km was summed until the total area was +6010 mgal·km: this value was reached at the distance +22 km. The distance +22 km was then chosen as a line of symmetry and a mirror image of the values of g_f south of the line was "reflected" to the north. The resulting curve is shown in figure 9(b). Curve 9(c) was constructed by subtracting 9(b) from 9(a). The manner of choosing 9(b) is responsible for the zeros between +20 km to -180 km; a more sophisticated manner of choosing 9(b) could shift the right hand side of 9(c) a bit to more nearly match the left hand side of the trench, but the uncertainties of this method don't warrant more than a simple treatment.

This separation of the gravity profile into two parts, a part by an "isostatic island" and a part by the "trench alone", enables us to ignore the complicating effects of the island. A complete theory of trenches would have to consider the neighboring islands: such islands are an intimate part of every trench. But such a theory would have to be evolutionary showing how the island slowly accreted until it reached its present size. Our less ambitious goal here is to recognize the existence of an island at present,

but to ignore how it came to be. We are interested only in the possible convective motions now in action which produce the present trench. However we may note that the total volume of crustal rocks beneath the trench and island are comparable to the volume which would be carried there if 1500 km of ocean floor had been drawn down into the trench and then deposited under Puerto Rico. If the ocean bottom drifted at the rate of 1 cm/yr, this would correspond to a time of 150 million years. Using the bottom profiles shown in figure 12 between the horizontal distances of +300 km and -100 km, the volume of rock of density 2.7 gm/cm^3 is 1920 km^2(x 1 cm) and of density 3.0 gm/cm^3, 7850 km^2 (x 1 cm). Assuming 5.5 km, 7.0 km, and 11.5 km to be the appropriate dividing lines in a typical ocean, we compute that a strip of ocean 1500 km long would have a total volume of lighter and heavier crustal rocks of 2250 km^2 (x 1 cm) and 6750 km^2 (x 1 cm) respectively. Thus we see how the simple model to be presented here might be extended into an evolutionary model.

Figure 10 shows the free air anomaly of the "trench only" of figure 9(c) together with two theoretical free air curves drawn using formula (35). The theoretical curves were computed for a cylindrical object sinking straight down beneath +170 km. The magnitudes and the widths of the theoretical curves were adjusted by changing the mass per unit length, M_L, and the depth, D, of the sinker. The two curves, which correspond to sinkers at 80 km and 90 km, show how well this three parameter theory agrees with the data (two parameter once the line of symmetry is chosen) and show approximate limits as to how much these parameters may be varied. I consider the D = 80 curve to be the better fit: the difference between this curve and the "trench only" curve is roughly a constant 20 mgal. and this constant offset could be caused by another, more general, feature. We have previously seen (section

Figure 10. The free air anomaly of the residual "trench alone" and two choices of the simple viscous model.

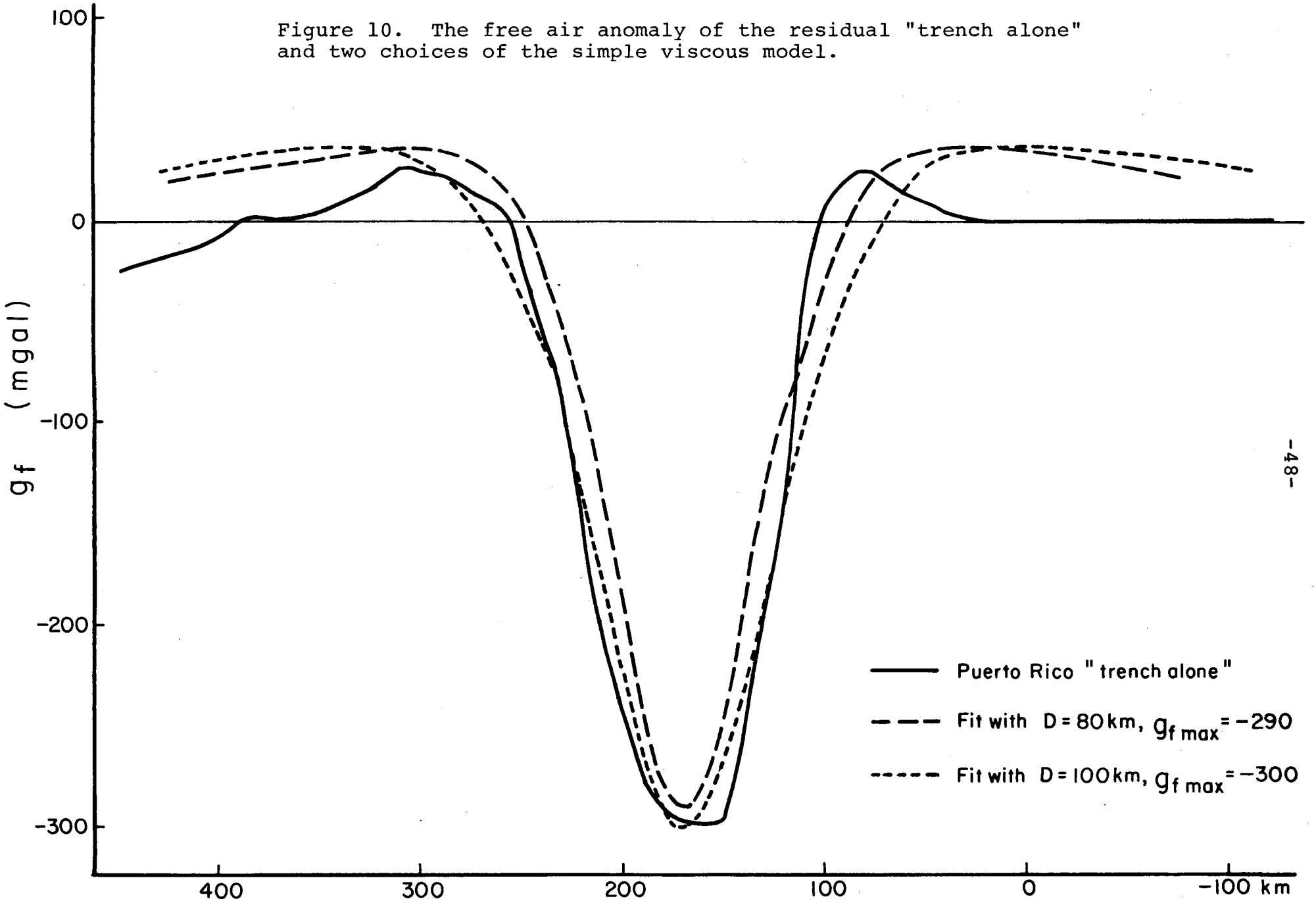

4) that with any pattern of viscosity the total mass deficit on the surface equals the mass excess below. This must be so in order that there is no motion involving the longest wavelength. The negative part of g_f just over the sinker is produced mainly by the viscous response to the sinking object and the shape of this part of the curve could be changed if the simple viscous relation were not valid, but the positive part of g_f on each side is produced by the gravitational attraction of the excess mass of the sinker. If the material has a finite strength (plastic) or if there are complicating features 100 km down which limit the sinking velocity in some way, these could only reduce the magnitude of the mass deficit on the surface. But less surface mass deficit, or more surface load, could only make the net line integral of g_f positive instead of zero. Any conceivable plastic or elastic change should only make the "wings" of the "trench only" curve more positive than is observed. The conclusion is that this area of the globe -- the Caribbean and Western Atlantic -- must have an average value of g_f which is less (by about 20 mgal) than standard. Indeed we observe that the geoid is depressed by about 10 meters in this region. (Kaula, 1964)

For the curve with D = 80 km we find that the mass per unit length of the sinking cylinder is $M_L = 1.7 \times 10^{13}$ gm/cm. If this mass excess is in a cylinder with a 40 km radius, the average excess density of the cylinder is $\Delta\tilde{\rho} = .34$ gm/cm^3, or 10% more than the average density of the upper mantle. We suppose that the sinker is much cooler than its surroundings since it has been brought down from the cooler top layers of the earth. The heating of this large blob by conduction or radiation transfer from the surrounding material would be a very slow process (see below) and the amount of heating caused by the adiabatic compression is negligible. For an order of magnitude estimate of the time required for a cylinder of radius 50 km

to heat up to an appreciable fraction of the temperature of its surroundings, consider the following simple argument. The equation for heat diffusion is $\nabla^2 T = \frac{k}{\rho c_p} \frac{\partial T}{\partial t}$ and we find from dimensional arguments a characteristic time, t_c. Using a=50 km, $\tilde{\rho}$ = 3.3 gm/cm^3, c_p = .2 cal/gm°C, and k = .006 cal/cm°Csec; we find that this characteristic time is $t_c = \frac{k a^2}{\rho c_p}$ = 100 million years. Thus, within perhaps a factor of three, we find that in 100 million years the temperature at the center of the cylinder will heat up by about one-half of the difference between the original temperature at the center and the temperature at the surface of the cylinder. This long time is required since heat transfer by conduction or radiative transfer is a very slow process compared to heat transfer in the earth by convection. (the k = .006 above was a total thermal conductivity, including the average effects of both of these processes). Thus if the sinker sank at a rate of 1 cm/year, it would require only 10 million years for the cylinder to sink to a depth of 100 km and the temperature change due to conduction inward from the surrounding medium would be negligible in this short time. Since the surface temperature is about 0°C and the temperature at 100 km is about 1500 °C in several proposed temperature models, a temperature difference of 1000 °C between the sinker and its surroundings could possibly exist although a much smaller temperature difference is more likely. If the density excess were due to linear thermal expansion with a volume expansion coefficient of $\alpha = 3 \times 10^{-5}$/°C, a 1000°C temperature difference would produce only a 3% change in the density, not the 10% change which we require. If however there is a phase transition, which could occur here at a much shallower depth than normal if the temperature here were several hundred degrees cooler than average, then this 10% density excess is within reason.

This required 10 % excess density could be reduced considerably if the sinker were at a greater depth than the 80 km which we found above with the simple viscous model since if the sinker were deeper the excess mass could be spread out more in a greater volume. We have seen (figure 6) that if the viscosity near the surface is very much greater than the viscosity at the depth of the sinker, then the shape of the curve $F_z(x)$ is changed somewhat. We have used the expression for $F_z(x)$ resulting from the uniform viscosity case, but if we used the form of $F_z(x)$ corresponding to say an upper layer with a viscosity ten times that below and the upper layer having a thickness one half of D, then the depth of the sinker for which the $g_f(x)$ curve best fits the "trench only" will be deeper than 80 km. The top part of figure 11 shows $g_f(x)$ calculated for a mass of $M_L = 1.7 \times 10^{13}$ gm/cm at a depth of D = 80 km for two choices of the shape of $F_z(x)$. Case (a) is for a thick layer on top having a viscosity ten times that below (R = 1/10, d/D = 1/2) and case (b) is for the simple uniform viscosity (R = 1). In the lower part of this figure, case (b) is the same as above (a mass at 80 km and the simple formula) and in case (c) the depth and mass of the layered model (R = 1/10, d/D = 1/2) have been adjusted to closely match this simple curve. This new fit gives a mass which is 87 % of the original mass and a depth which is 25 % greater than the original 80 km, or 100 km. Notice that we could have chosen R = 1/100 or 1/1000 with very little additional changes in the shape of $F_z(x)$. Further, the effects of the ratio d/D seem to be approaching a limit (see figure 6). We have introduced an additional set of parameters into the model, but the effect of these changes is very slight. We would predict essentially the same mass beneath the surface with almost any variation of R and d/D, and we would have a range of depths D varying about 30 % depending on the choice of R and d/D.

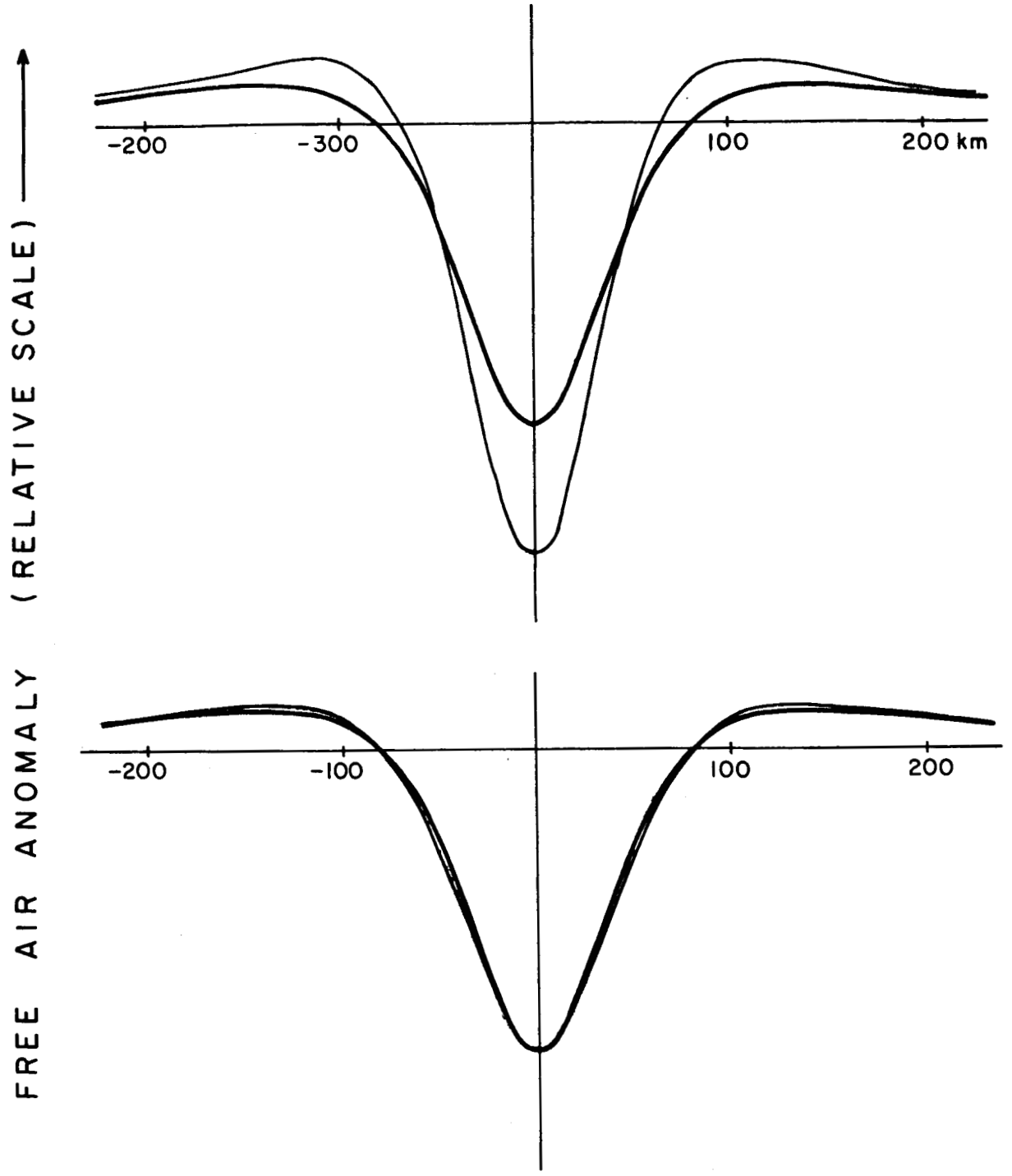

Figure 11. A comparison of the free air anomaly calculated with the simple viscous model and with the two layer model with R = .1 and d/D = .5.

(a) Simple viscous model, D = 80 km, M = 1.7 x 10^{13} gm/cm
(b) Two layer model, D = 80 km, M = 1.7 x 10^{13} gm/cm
(c) Two layer model, D = 100 km, M = 1.5 x 10^{13} gm/cm

We shall accept the results of the modified simple viscous model and suppose there is a cylindrical mass of 1.5×10^{13} gm/cm located 100 km beneath the horizontal distance +170 km. If this is so then the Moho M as shown in figure 7 is incorrect and we must find the new bottom profile M'. A two-dimensional gravity anomaly program as described by Talwani, Worzel, and Landisman (1959) was used. Only two changes were made in the structure shown in figure 7: a mass was added at 100 km and the bottom surface of the 3.0 gm/cm^3 layer was adjusted so that the gravity anomaly of the difference between M and M' canceled the attraction of the deep mass. It was required that the curve M' have a depth of 11 km at +320 km. Excepting the constant offset introduced by requiring the curve to pass through a given point, the residuals of the final fit were less than 2 mgal. The resulting bottom curve M' is shown in figure 12(a). The original curve M is also shown for reference.

There is considerable discrepancy between M' and the seismic depths beneath the Venezuelan Basin and the following changes were made in the assumed upper structure in order to bring the gravitationally calculated Moho and the seismic Moho more in line. There is some freedom in the location of the layer interfaces beneath the Venezuelan Basin and each of these was moved upward approximately .5 km. The narrow finger of mantle reaching up at +100 km is probably not real but rather reflects an error in the thickness of the upper layers. The 3.8-5.5 km/sec boundary was adjusted between +120 km and +60 km in a manner to remove the need for this narrow finger of mantle. The Moho was recalculated after these changes in the upper layers at +100 km and between -100 km and -200 km were made. The new bottom profile was called M" -- it is shown in figure 12(b).

The Moho under the Venezuelan Basin is still too shallow. We may further lower the profile M" here if we remove a simplification made by

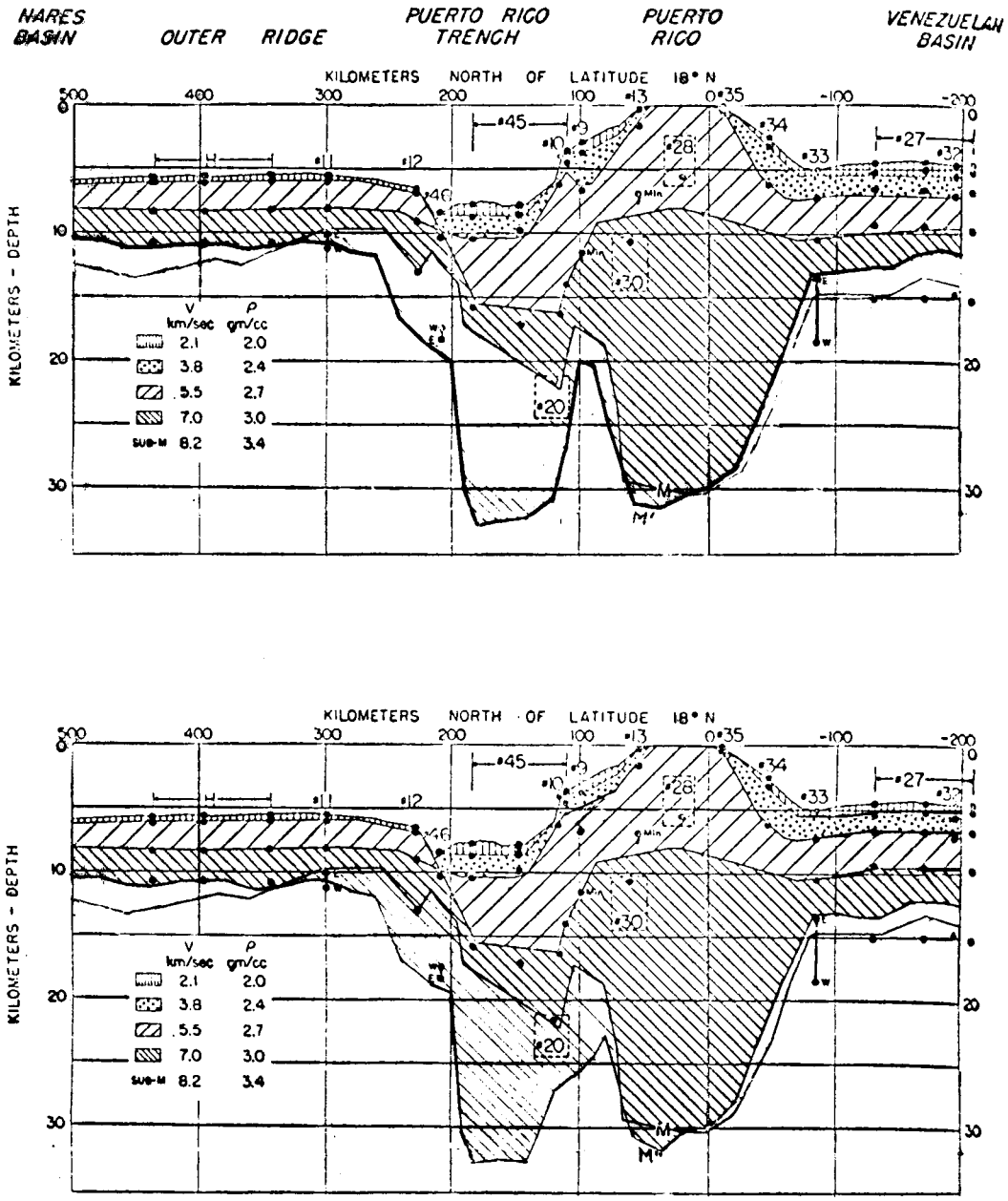

Figure 12. The Moho computed assuming there is a cylindrical mass of 1.5 x 10^{13} gm/cm at 100 km depth beneath horizontal distance +170 km. (a) The upper structure is the same as shown in figure 7. (b) The upper structure has been changed near +100 km and between -100 and -200 km.

Talwani, Sutton, and Worzel. These authors assumed there were only five different layers having velocities 8.2, 7.0, 5.5, 3.8, and 2.1 km/sec and densities 3.4, 3.0, 2.7, 2.4, and 2.0 gm/cm^3 respectively. These velocities are not the velocities observed beneath the Venezuelan Basin. Cross-sections summarizing the seismic results given in Officer et al (1959) (cross-sections 1 and 3) show a difference between the Caribbean and Atlantic side of the Puerto Rico Trench. Velocities of 8.1, 7.2, and 6.3 km/sec are more typical of this region than 8.2, 7.0, and 5.5 km/sec. From the Nafe and Drake velocity-density curve given in figure 2 of Talwani, Sutton, and Worzel (1959), these velocity differences correspond to density differences of -.03, +.07, and +.17 gm/cm^3 in the mantle, high velocity basement ("7.0") and low velocity basement ("5.5"). If Talwani, Sutton, and Worzel had used these greater densities for the "5.5" and "7.0" layers, the Moho M would have been placed 2 kilometers deeper than shown in figure 7. The extra density in these layers would have been compensated for by having a thicker crust. Thus if we make this correction to M (add 2 kilometers) and hence to M' and M", the resulting gravity curve for the Moho will pass through the points determined seismically. If the density beneath the Moho in the Venezuelan Basin were decreased as indicated by the 8.1 km/sec velocity, the amount of downward displacement of the Moho as described above would be lessened. If this lighter mantle were 10 km thick, this correction would be reduced from 2 km to 1 1/3 km.

We now look at the central portion of the figure; the seismic depth to the Moho as determined by lines 12, 46, and 20. Seismic profile 20, 1956 cruise, as given in Officer et al, 1959, places an interface between the 5.5 km/sec layer and a 6.8 km/sec layer at 18 km and an interface between the 6.8 km/sec layer and a 8.4 km/sec layer at 22 km. The 6.8

km/sec layer was "masked"; that is a straight line representing this layer was not observed in the travel time diagram but such a layer could be present. There is scatter in the travel time diagram and the 8.4 km/sec velocity depends critically upon which data points the straight line is drawn through. Another line may be drawn through to fit these points which gives a 7.2 km/sec velocity. Thus profile 20 could be reinterpreted to give a transition from 5.5 km/sec to 7.1 km/sec at a depth of 18 km with the Moho unobserved. This seismic profile has more scatter in the observations determining the deepest layer than most of the other profiles and it cannot be used as strong evidence against having the Moho deeper than 22 km.

Profiles 12 and 46 are presumably accurate measurements of the Moho. The depth to the Moho predicted by the viscous model (figure 12) is in disagreement with these points. This contradiction cannot be removed unless horizontal gradients in the viscosity are introduced. If we remove the symmetry of the problem -- that is let the deep mass be further to the south, say at +140 km, and the vertical load near the surface still be centered about +170 km -- then the Moho so determined could pass through the points given by profiles 12 and 46 with little change in the rest of the picture.

To summarize, we may dynamically account for the existence of the Puerto Rico Trench by supposing there is a cylindrical sinker approximately 80 or 100 km beneath the trench. We have seen that the variation of viscosity with depth is unimportant, especially if the viscosity increases towards the surface. If we calculate the magnitude of the stresses involved from formula (35), we find that the shear stresses have a maximum of roughly 500 bars and that we have stresses greater than 10 % of this over several hundred kilometers. These large stresses should exceed any brittle strength of the

material and viscous type flow result. If the driving mass is 1.7×10^{13} gm/cm and is distributed in a cylinder with a radius of 40 km, then this cylinder must have a density of .3 gm/cm^3 or 10 % greater than the surrounding density. If a driving mass of 1.5×10^{13} gm/cm is distributed in a cylinder with a radius of 50 km, then the average density excess is 5 % greater than the surrounding material. There is probably not a sharp transition between crustal material of density 3.0 gm/cm^3 and mantle material of density 3.4 gm/cm^3, but if there is the Moho would have a shape roughly as shown in figure 12(b). The upward bend in M'' near +100 km probably results from an error still remaining in the assumed structure of the upper crust; the discrepancy between M'' and the seismic measurements beneath the Venezuelan Basin can be accounted for by changing the density of the upper layers.

We now turn to the Mid-Atlantic Ridge. Figures 13, 14, and 15 show a map of the region considered, gravity anomalies and the crustal structure of the ridge, and some proposed crustal models. These three figures are from Talwani, Le Pichon, and Ewing (1965). In Puerto Rico the seismic crustal data was lacking in the critical region from +100 km to +200 km and only free air gravity anomalies were used to locate the size and depth of the sinker. In the Mid-Atlantic there is sufficient crustal structure information so that the vertical load and subcrustal anomaly may be used as well as the free air anomaly. The depth to the Moho is lacking within $\pm$ 300 km of the center of the ridge, but crustal data in the 300 to 1000 km range will be useful.

The top part of figure 16 shows the Bouger anomaly and the subcrustal anomaly. The Bouger anomaly shown was obtained by drawing a smooth curve through the Bouger curve shown in figure 14 and recording the value so found

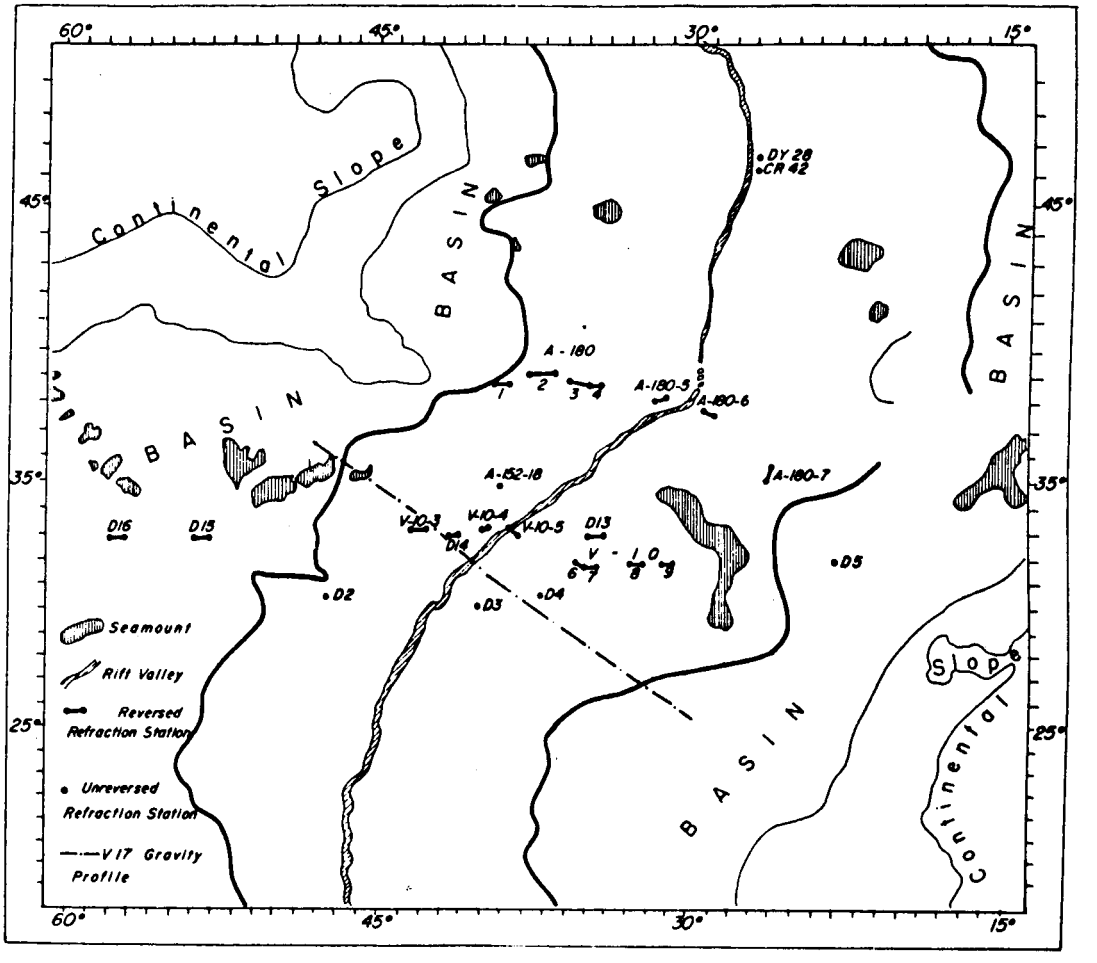

Fig. 1. Location of seismic refraction measurements on north mid-Atlantic ridge between latitudes 20°N and 50°N. The track of *Vema* cruise 17 during which continuous gravity measurements were made is also shown.

Figure 13. (From Talwani, Le Pichon, and Ewing; 1965)

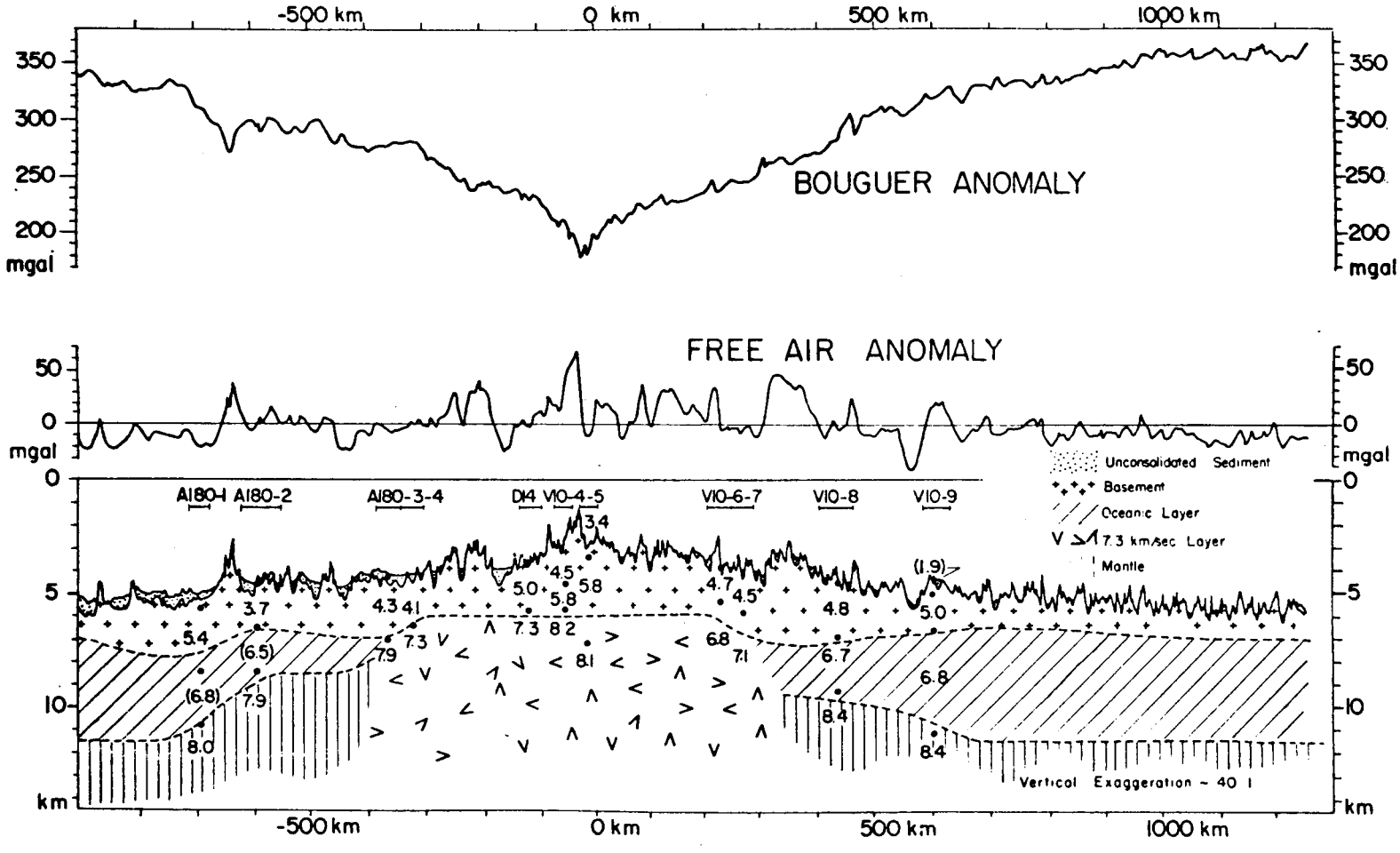

Fig. 2. Gravity anomalies and seismically determined structure across the north mid-Atlantic ridge. The continuous gravity data were obtained on *Vema* cruise 17. Bouguer anomalies were obtained assuming two dimensionality and assuming a density of 2.60 g/cm^3 for the basement layer. A correction was also made for the sediment layer. The seismic section is obtained by projecting the structure at seismic stations along the gravity profile. Seismic horizons are represented by dots. Values of compressional wave velocities in km/sec are indicated. Numbers within parentheses denote assumed seismic velocities.

Figure 14. (From Talwani, Le Pichon, and Ewing; 1965)

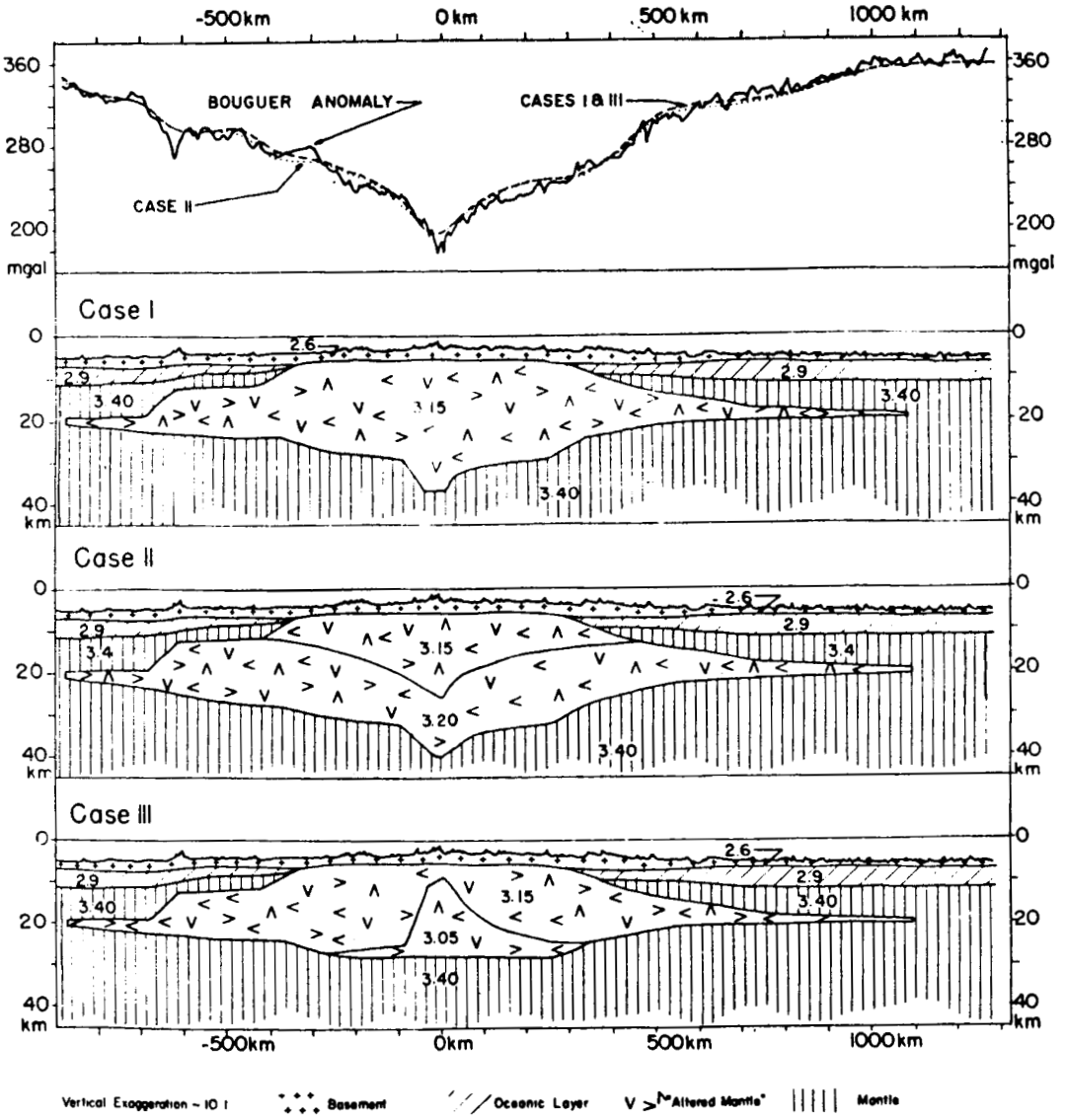

Fig. 5. Three possible crustal models across the north mid-Atlantic ridge which satisfy gravity anomalies and are in accord with seismic refraction data. In all three models the anomalous mantle found seismically under the crest of the ridge is assumed to underlie the normal mantle under the flanks of the ridge. In case I the anomalous mantle is assumed to have a uniform density; in case II its density is assumed to increase downward, and in case III the material constituting the anomalous mantle is assumed to be lighter near the axis of the ridge.

Figure 15. (From Talwani, Le Pichon, and Ewing; 1965)

every 100 km. A constant was subtracted to make the curve zero at +1200 km. The subcrustal curve was found by adding a correction to the Bouger curve which depends on the thickness of the crustal layers below. The depths to the interfaces were taken every 100 km from figure 14 and densities of 2.6, 2.9, 3.4, and 3.15 gm/cm^3 were assigned to the layers (the same densities as shown in figure 15). It was assumed that the anomalous 3.15 gm/cm^3 layer ended at 11.5 km for the purpose of this calculation. If this 3.15 layer extended deeper than 11.5 km in the range -400 km to +300 km, the curve g_s would be flatter in the center or even bend up the opposite way. That is, if there is more light material near the surface, the subcrustal anomaly curve g_s would be less negative showing that less light material is needed down deep.

In the models proposed by Talwani, Le Pichon and Ewing (figure 15), it is assumed that the crustal structure is as shown in figure 14 and that all differences between the observed gravity and the gravity anomaly computed using this crustal structure are caused by masses below. They have been forced to place these subcrustal masses at about 20 km depth because they require the subcrustal mass to account for <u>all</u> of the residual anomaly. In particular, at -650 km they have a sharp change in the thickness of their subcrustal layer which is to account for the sharp change in the Bouger anomaly (or g_s) at -650 km. If we look at the structure shown in figure 14 we see that this change in g_B is caused by the seamounts at -650 km. The depth to the Moho shown here was determined by seismic profiles A180-1 and A180-2 and we see from the map in figure 13 that these depths were measured more than 500 km to the northeast. There is probably a root under this seamount and although g_B (water-basement) does have a sharp change at

-650 km, g_s (all crust including root) should not have this sudden change. It will be assumed from here on that the departures of g_s in the range from -700 km to -400 km are caused by errors in the assumed crustal structure. We assume that if the root under the seamount were inserted and other changes made between -600 km and -400 km, then the resulting g_s curve would be symmetric about the center.

If we allow the possibility of changes in the profiles of the crustal structure, then the subcrustal mass deficiency need not be around 20 km down. For example, all of the mass deficiency may be concentrated in a line source 400 km deep. Figure 16(b) shows g_s and the gravity due to a source at 400 km; figure 16(c) shows the difference between these two curves. If we examine only the right hand side of figure 16(c), we see that a single mass at 400 km could well account for most of the mass deficiency beneath the ridge. The approximately 20 mgal fluctuations in the "g_s - 400" curve could be accounted for by irregularities in the profile of the Moho. With the density contrast of 2.9 - 3.4 gm/cm^3, a change in the depth of the Moho alone of 1 km would result in a 20.9 mgal change in the gravity anomaly. If both the Moho and the 2.6 - 2.9 gm/cm^3 interface changed by 1 km, the gravity anomaly would change by 33.5 mgal. The possibility of bottom fluctuations of this magnitude cannot be discounted, at least not until many more seismic measurements have been made on the ocean floor. Thus the light mass required to counterbalance the gravitational attraction of the ridge itself may be at almost any depth. The distribution at about 20 km shown in figure 15 and the single line source at 400 km are extreme cases: the lighter mass is more likely to be somewhere in between.

From the subcrustal anomaly we know there is lighter than average material beneath the ridge, but from this anomaly alone we cannot specify

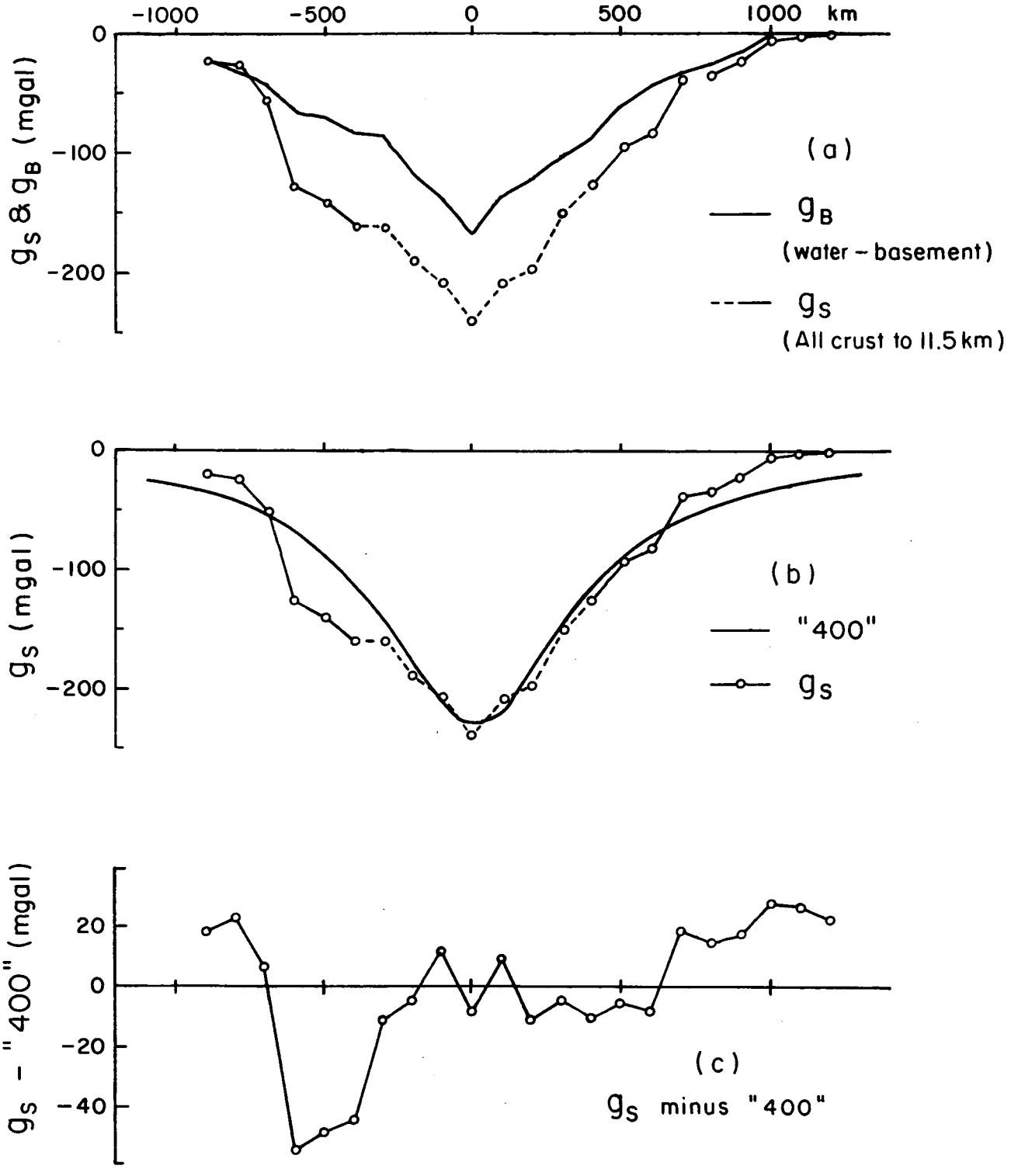

Figure 16. Gravity anomalies over the Mid-Atlantic Ridge.
(a) The Bouger anomaly and the subcrustal anomaly as described in the text.
(b) The subcrustal anomaly and the anomaly computed by assuming a line source 400 km beneath the center of the ridge.
(c) The difference between the curves shown in (b).

the density pattern with depth. However if we trust the viscous model, we may find the mass deficiency below which will maintain the ridge in its elevated state. Figure 17 shows the subcrustal anomaly and the vertical load and free air anomaly computed with the simple viscous model for each of the density distributions shown in figure 18. In (a) we have the effects of a cylindrical source 400 km beneath the center of the ridge. In (b) we have taken that mass distribution at 200 km for which the g_s will exactly match the g_s of a cylindrical mass at 400 km. The g_s is the same in (a) and (b); the F_z and g_f are different. In (c), we have chosen a mass distribution at 100 km which closely fits the observed g_s (or rather the right hand side of g_s since we are ignoring the left hand side). The computed values of g_f are too large in this model and there is considerable unknown in g_s since we do not know the depth of the 3.15 gm/cm^3 layer in the center of the ridge; and so in (d) we have chosen a mass pattern at 100 km depth which better fits g_f in the center of the ridge and is the same as before for the outer flanks. In (e), we have the same mass distribution except it has been raised from 100 km to 80 km. Notice how this reduces the free air anomaly by about 20 %.

The right hand side of these symmetric mass distributions are shown in figure 18. In parts (b) through (e), the density deficiency is .03 gm/cm^3 or 1% less than the average density at this depth. For the purpose of the calculations, it was assumed that all of the mass was concentrated at 200, 100, or 80 km. The thickness of the light layer was drawn in after choosing a density difference between the lighter layer and its surroundings. The values of F_z and g_f shown in figure 17 were calculated with the simple viscous model. If the modified viscous model had been used, partially

taking into account the increase of viscosity towards the surface, the masses would have been slightly smaller and about 20 % deeper.

In conclusion, the mass inhomogeneities which drive the Mid-Atlantic Ridge are at about the same depth as those which drive the Puerto Rico Trench -- 100 km. The density deficiency of this driver is about 1% beneath the ridge; this could arise from a temperature difference if the mantle beneath the ridge were about 300°C warmer than average at this depth. This contrasts to the Puerto Rico Trench where the density excess of the driver was 5% or more -- a magnitude which could arise only from a phase change or chemical differentiation. The horizontal motion of the surface of the ridge cannot be predicted since horizontal features depend critically upon the assumed vertical layering of viscosity, but the shape of the ridge and the magnitude of the free air anomaly can be predicted by the viscous model in a manner independent of detailed assumptions of the viscosity pattern.

Figure 17. The observed values of the subcrustal anomaly g_s, the vertical load F_z, and the net free air anomaly g_f, of the Mid-Atlantic Ridge and theoretical values computed from a model.

(a) In this model all of the mass deficiency was concentrated in a line source at a depth of 400 km. See figure 18(a).

(b) The mass deficiency was distributed at a depth of 200 km in a manner to exactly match the g_s of the line source at 400 km. See figure 18(b).

(c) The mass deficiency was distributed at a depth of 100 km in a manner to closely match the observed g_s points. See figure 18(c).

(d) The mass deficiency was distributed at a depth of 100 km. The amount of mass is less in the central portion in order to more closely fit the observed g_f rather than the more speculative g_s. See figure 18(d).

(e) The same as above, except at 80 km. See figure 18(e).

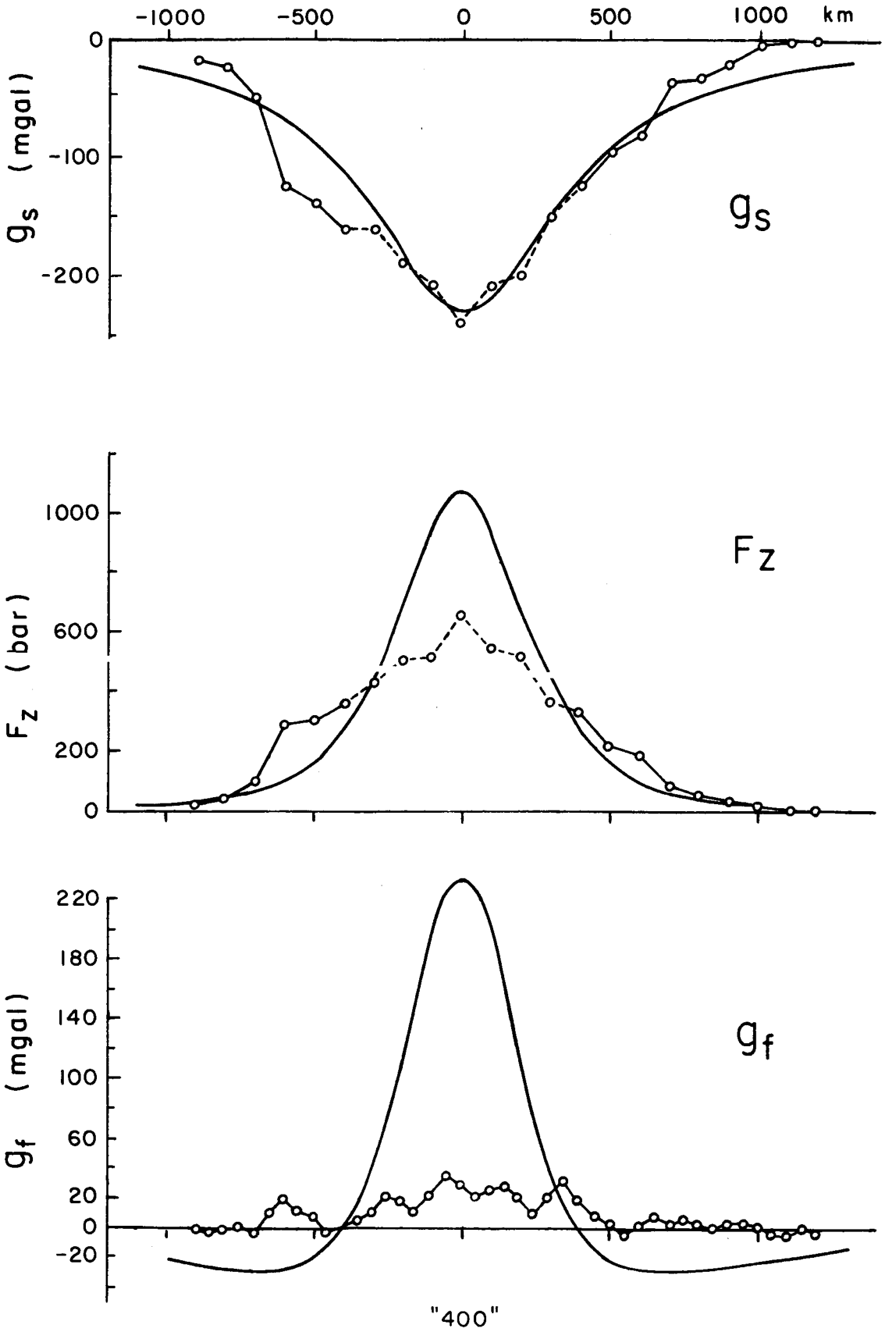
-1000
-500
0
500
1000
km
0
-100
-200
g_s (mgal)
g_s
1000
600
200
0
F_z (bar)
F_z
220
180
140
100
60
20
0
-20
g_f (mgal)
g_f
"400"

Figure 17(a).

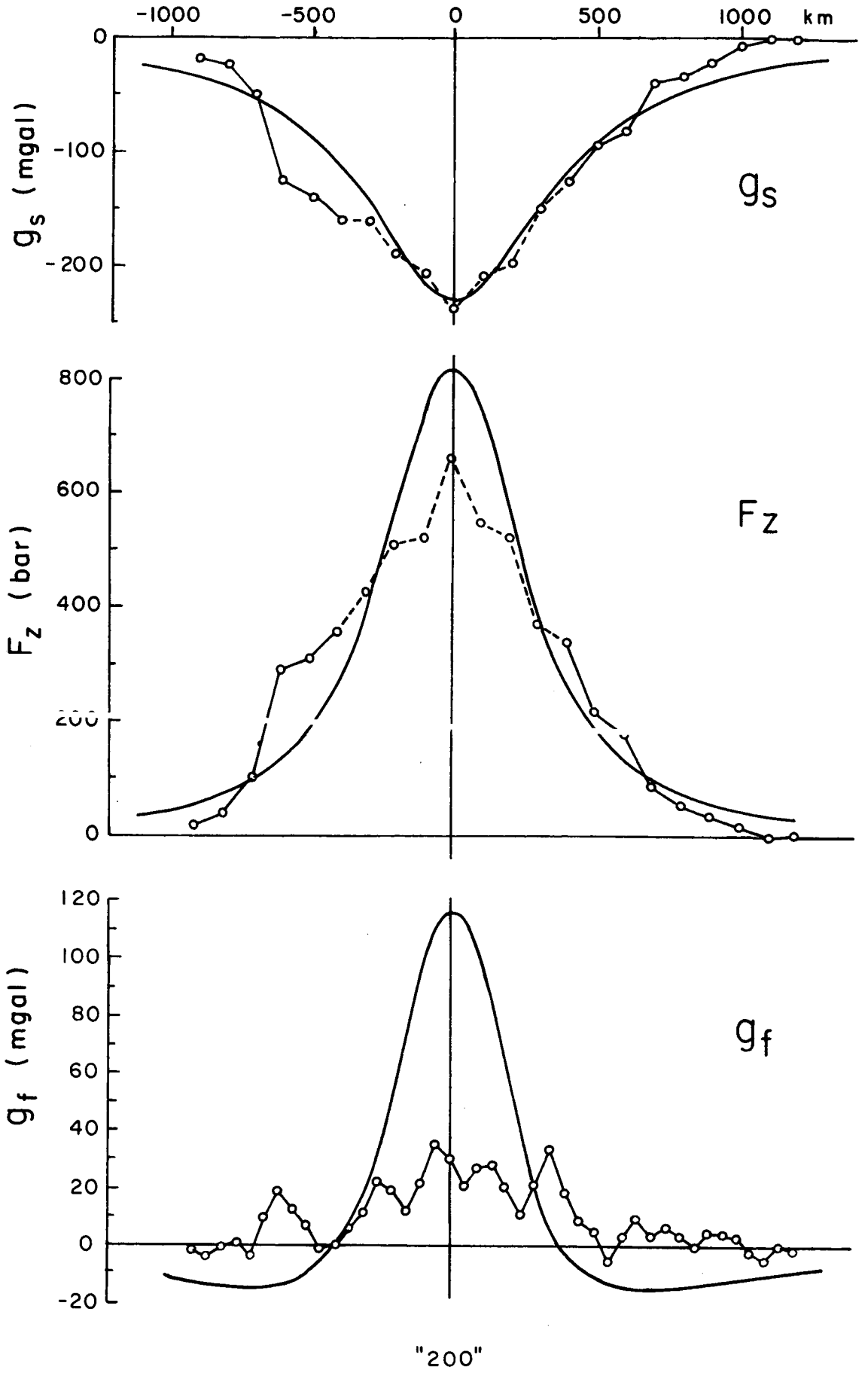

"200"

Figure 17(b)

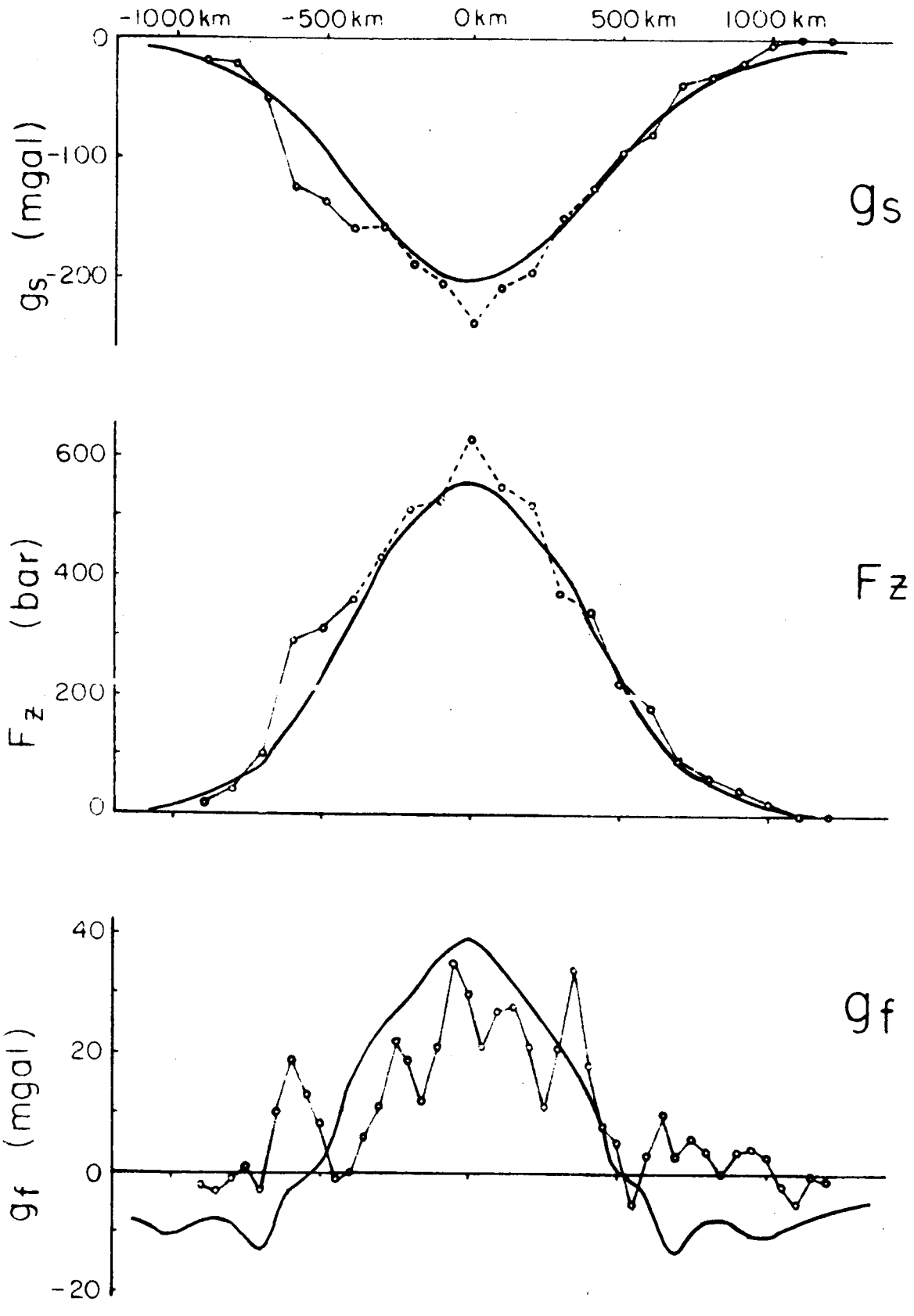

"100"

Figure 17(c)

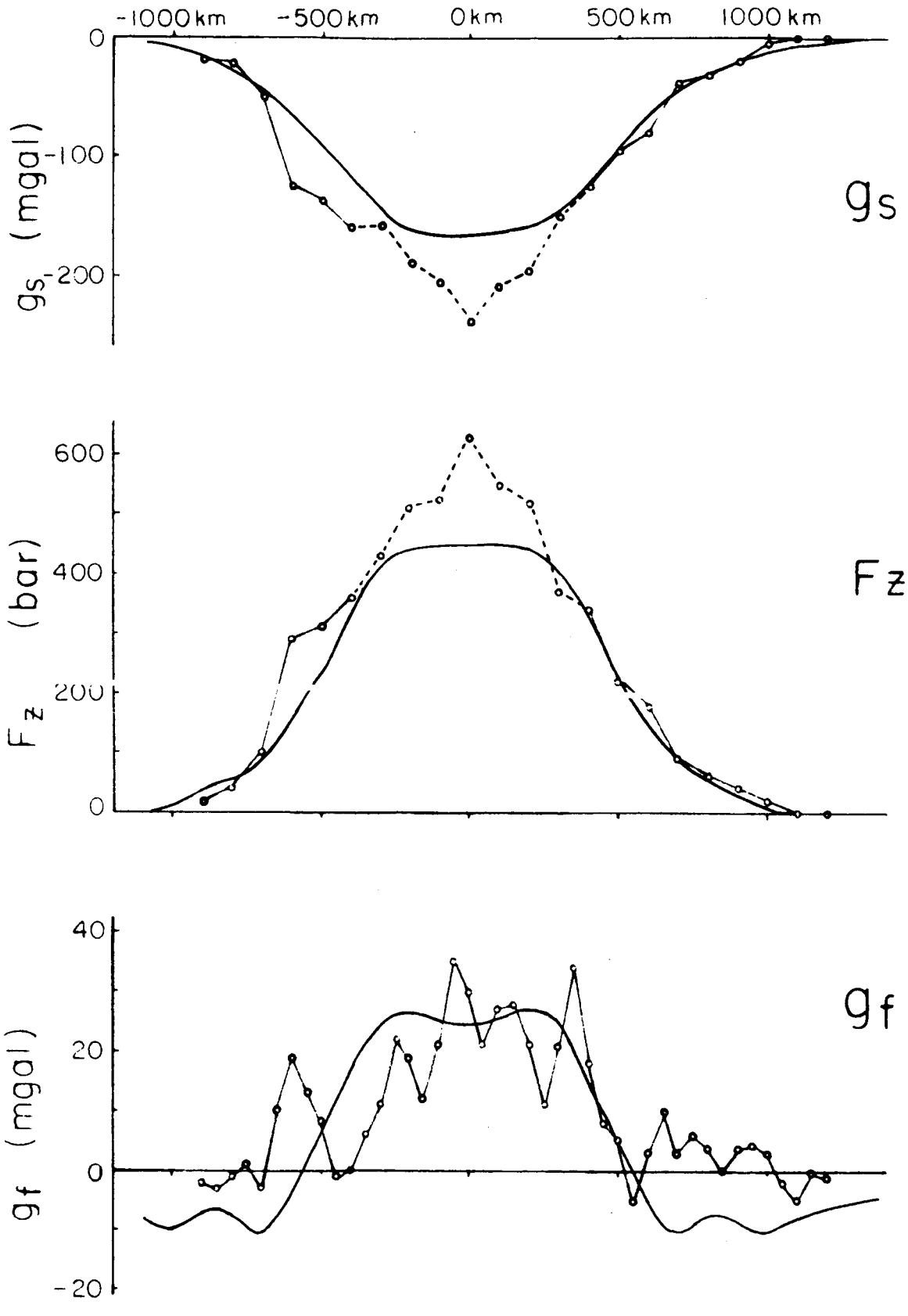

"100 C"

Figure 17(d)

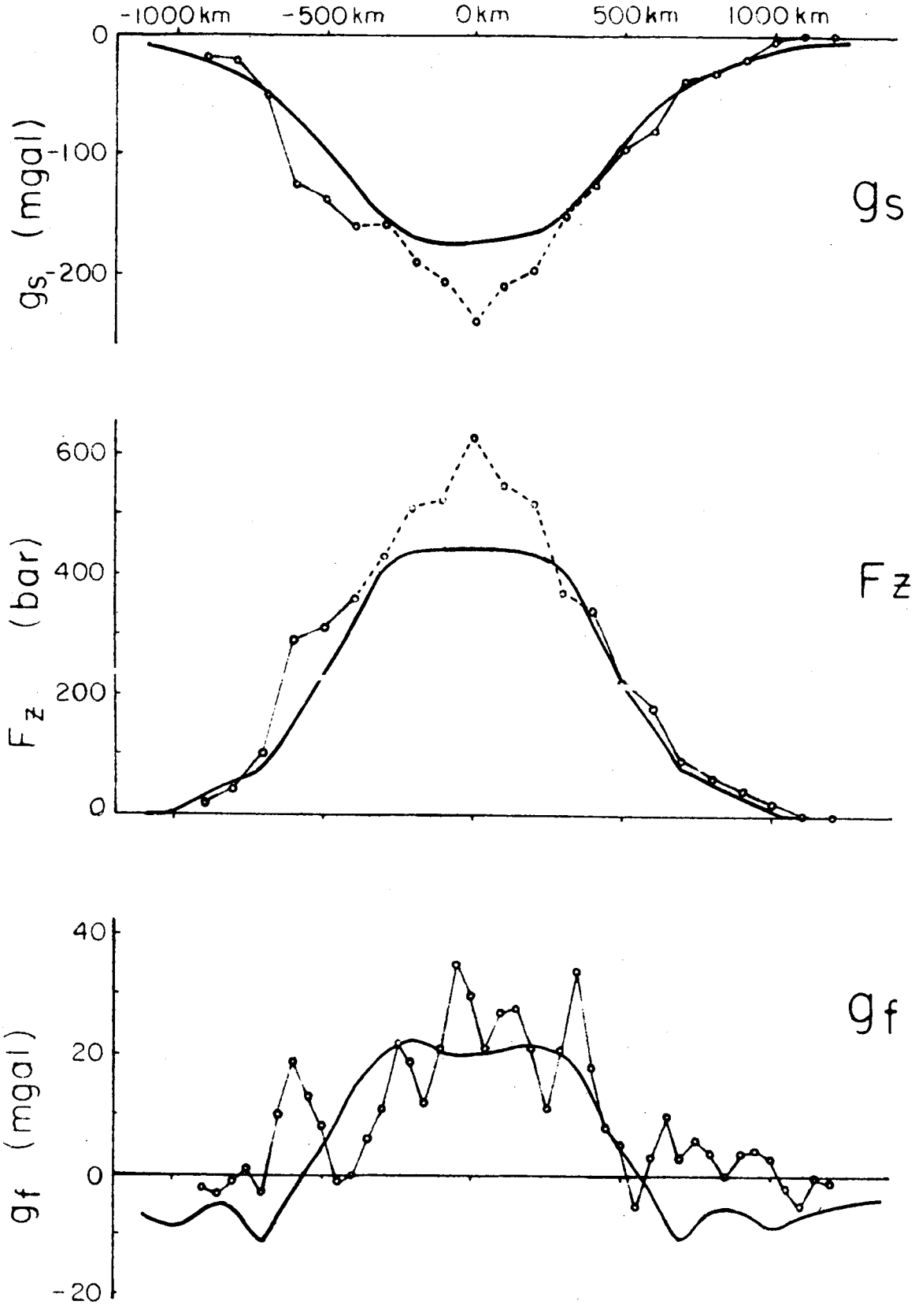

"80 c"

Figure 17(e)

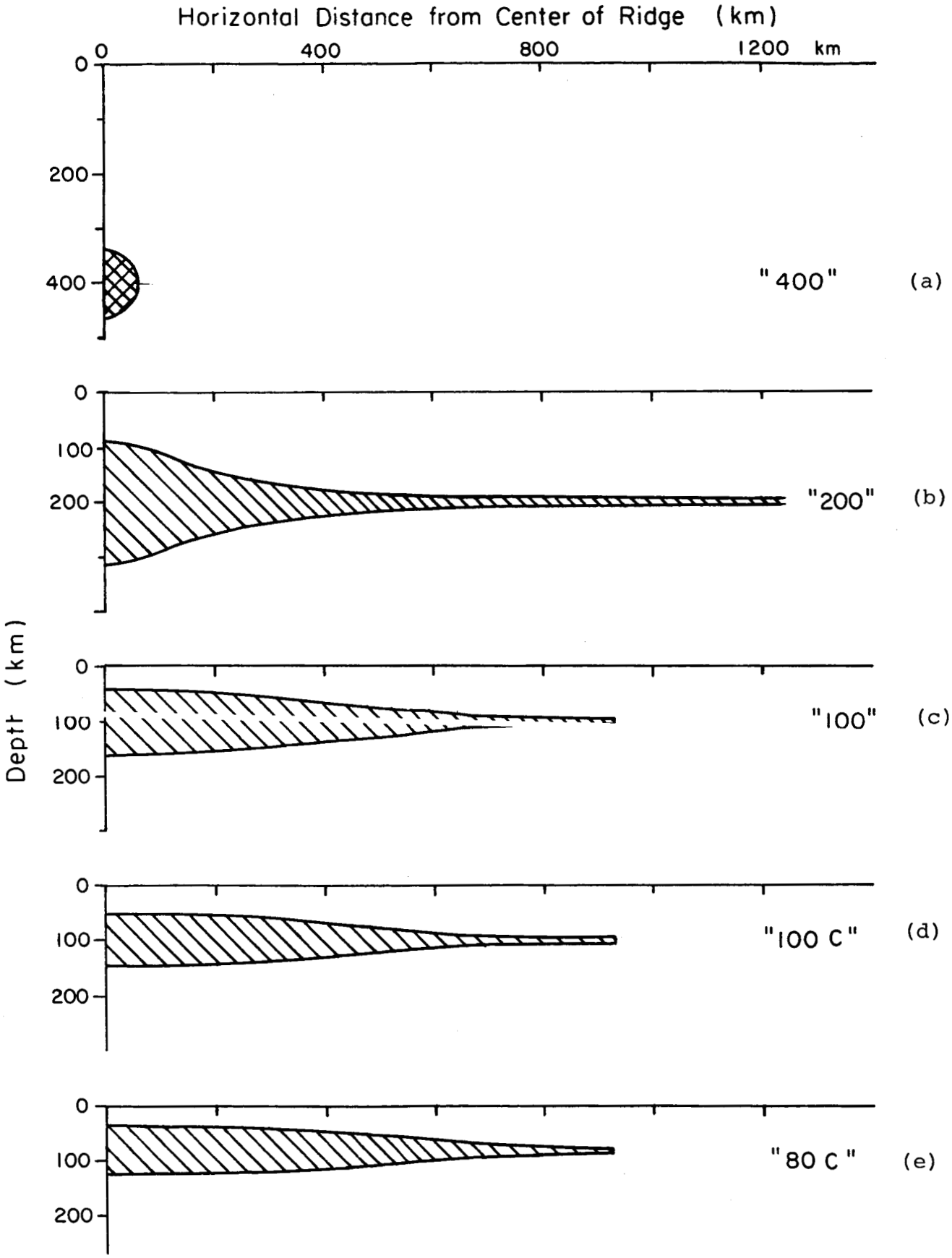

Figure 18. The two-dimensional mass distributions which produce the effects shown in figure 17. The mass deficiency of the cylinder in (a) is 6.9×10^{13} gm/cm. The density deficiency within the shaded areas of the last four models is .03 gm/cm^3 or 1% less than the surrounding material.

Acknowledgements

I wish to thank Professor W. M. Elsasser for suggesting this problem and for his continued interest. Without his comments and suggestions this paper would not have been completed in its present form.

I also thank Professors H. H. Hess and W. E. Bonini for directing me to sources of gravity measurements and aiding me in their interpretation. I thank Professor Bonini again for showing me how to use the two-dimensional gravity computer program. I thank Dr. B. R. Durney for his help with the solution of some of the mathematical problems.

Dr. J. L. Worzel of Lamont Geological Observatory kindly showed me a large number of preliminary continuous gravity profiles across trenches in the Pacific. The variety in these profiles led to a change in emphasis in this report; from a primary interest in the horizontal velocity to a concentration on the vertical load.

References.

Berker, R., Mouvement d'un fluide visqueux incompressible, Handbuch der Physic VIII/2, page 252, Springer-Verlag, Berlin, 1963

Cook, M. A., Viscosity-depth profiles according to the Ree-Eyring viscosity relations, J. Geophys. Res., 68, 3515-3520, 1963.

Eisasser, W. M., Thermal structure of the upper mantle and convection, unpublished report, 1964.

Faxén, H. (with an appendix by H. Dahl), Gegenseitige einwirkung zweier kugeln, die in einer zahen flüssigkeit fallen, Arkiv för Matematik, Astronomi och Fysik, A19, N:o 13, 1925/27.

Gutenberg, B., Changes in sea level, postglacial uplift, and mobility of the earth's interior, Bull. Geol. Soc. Am., 52, 721-772, 1941.

Haskel, N. A , The motion of a viscous fluid under a surface load, Physics, 6, 265-269, 1935.

Kaula, W. M , Determination of the earth's gravitational field, Rev. Geophys., 1, 507-552, 1963.

Lamb, H., Hydrodynamics, 6 ed., Cambridge University Press, London, 1932.

McConnell, R. K. Jr., Comments on letter by H. Takeuchi, 'Time scales of isostatic compensation', J. Geophys. Res., 68, 4397-4398, 1963.

Niskanen, E., On the upheaval of land in Fennoscandia, Isostatic Inst. Intern. Assoc, Geod. Publ. no. 6, Helsinki, 1939.

Officer, C. B., J. I. Ewing, J. F. Hennion, D. G. Harkrider, and D. E. Miller, Geophysical investigations in the eastern Caribbean: Summary of 1955 and 1956 cruises, Physics and Chemistry of the Earth, 3, Pergamon Press, London, 1959.

Orowan, E., Continental drift and the origin of mountains, Science, 146, 1003-1010, 1964.

Runcorn, S. K., Satellite gravity measurements and a laminar viscous flow model of the earth's mantle, J. Geophys. Res., 69, 4389-4394, 1964.

Takeuchi, H., and Y. Hasegawa, Viscosity distribution within the earth, to appear in J. Geophys. Res., 1965.

Talwani, M., X. Le Pichon, and M. Ewing, Crustal structure of the mid-ocean ridges, 2, Computed model from gravity and seismic refraction data, J. Geophys. Res., 70, 341-352, 1965.

Talwani, M., J. L. Worzel, and M. Landisman, Rapid gravity computations for two-dimensional bodies with application to the Mendocino submarine fracture zone, J. Geophys. Res., 64, 49-59, 1959.

Talwani, M., G. H. Sutton, and J. L. Worzel, A crustal section across the Puerto Rico trench, J. Geophys. Res., 64, 1545-1555, 1959.

Vening-Meinesz, F. A., The determination of the earth's plasticity from the post-glacial uplift of Scandinavia, isostatic uplift, Proc. Ned. Akad. v. Wetensch., Amsterdam, 44, 1, 1941.